SSCL-635

SSCL-635
July 1993
Distribution Category: 400

A. Spindel

Report on the Program of 4 K Irradiation of Insulating Materials for the Superconducting Super Collider

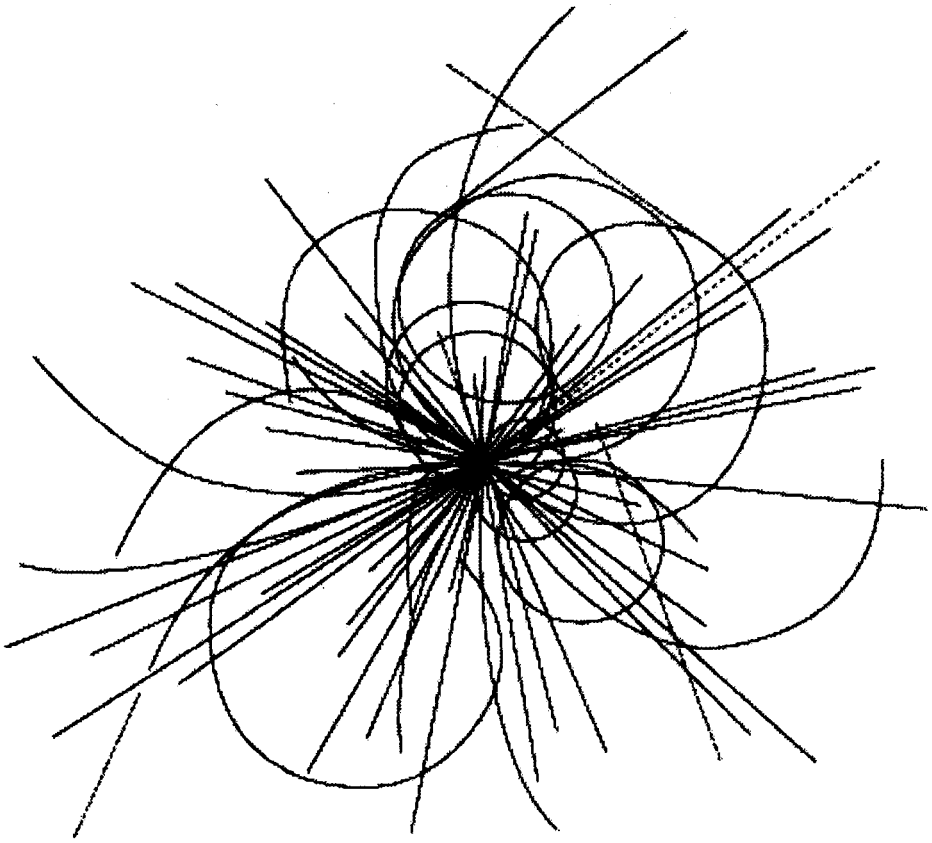

Superconducting Super Collider Laboratory

SSCL-635

Report on the Program of 4 K Irradiation of Insulating Materials for the Superconducting Super Collider

A. Spindel

Superconducting Super Collider Laboratory*
2550 Beckleymeade Ave.
Dallas, TX 75237

July 1993

*Operated by the Universities Research Association, Inc., for the U.S. Department of Energy under Contract No. DE-AC35-89ER40486.

1.0 INTRODUCTION

How to Use This Report

This report is intended to serve as an aid to material selection. The results reported herein are the product of a careful investigation and can be used with confidence in their validity. The selection of materials based on this data, however, is not the responsibility of the author. This report will not approve or disapprove any specific material for use in the Super Collider. The author of this report does not assume any design responsibility or responsibility for material selection for any application. It is, therefore, very important that those with design responsibility use this report wisely. For this reason, the following informational guide to the material selection process has been provided.

There are several issues to take into account when evaluating a material for radiation resistance. It is very important that the design criteria and operating loads for the application be known. For many applications the actual loading, and therefore required properties, are unknown. Certain materials have empirically been used successfully in a similar application and those materials have often been selected on that basis. Given the requirement that polymers and polymer matrix composites are not to be used to more than 40% of their ultimate strength, it is advisable that the actual loading be known so that it can be compared to the ultimate strength after irradiation and that compliance with this requirement can be demonstrated.

Both percent degradation and the magnitude of the actual properties after irradiation need to be considered. Consider the scenario where two materials are being compared that both have acceptable properties after exposure to 10^9 rads. One material was very strong initially and lost a significant proportion of its original strength to failure and had significant weight loss. The other material was initially less strong, but has not degraded appreciably. It is preferable to choose the material with less degradation because degradation tends to be a threshold phenomena with properties declining rapidly with dose after a certain threshold dose. The properties of the initially strong material, therefore, will be extremely sensitive to dose in that dose range and slight magnet-to-magnet differences in dose may, depending on the application, lead to performance variations. Also, because a slightly higher dose may cause the properties to degrade to unacceptable values, there is an inherent risk of using materials whose properties change dramatically.

2.0 BACKGROUND

Mechanical insulation failure has been reported as the most common cause of in use magnet failure in fusion magnets.[1] Studies of failure modes of accelerator magnets have generally been on prototypes. In use failures have not generally been investigated. Since an accelerator has to have high reliability and is a serial machine, the mechanical properties and loads of the parts have to be known in order to estimate the lifetime of the components. Additionally, the change in properties due to irradiation must be known and taken into account during design to guarantee sufficient performance at the end of the designed magnet life. Many, but not all of the materials under consideration have been studied for radiation damage, including Kapton,[1–6] Vespel,[1,7] Spaulrad,[1,8,9] G10CR and G11CR,[4,10] Isaryl,[11] PEEK[5,6] and Ultem.[5] Due to the nature of polymeric materials, the irradiation temperature, storage temperature, and testing temperature can all have an effect on the results of the test. Because the damage induced by radiation depends on the conditions of the experiment, it has been recommended that tests be performed to reflect the in-use conditions as closely as possible.[12–15]

Radiation causes damage to polymers and polymer matrix composites by a variety of mechanisms. A high energy photon (gamma, γ) or electron (e^-) will interact by Compton scattering, pair production, or by depositing energy into breaking bonds producing free radicals. Because the mechanisms are the same, and because the gammas undergo reactions that produce free electrons and vice versa, the term "electromagnetic showers" is used to describe the effects of γ and e^- radiation. It is not expected that there will be any difference in γ and e^- radiation on materials, and in fact several researchers[1,16,17] have found no difference between γ and

e^- damage or any difference in damage due to electrons at different energies.[18] The other prevalent type of irradiation is neutron irradiation. Neutrons tend to produce primary knock-on atoms, which tend to be hydrogen atoms selectively, which recoil and cause ionization. Elastic scattering of neutrons can form radicals. Neutrons also react with boron to form ^7Li and an alpha particle which causes further damage.[19] There have been several attempts at equivalent damage conversion from neutron fluence to absorbed dose of γ and e^-. [1,2,17,20] There is always a reported difference between the two, and conversions are inexact. In the Collider, 90% of the dose is expected to be due to electromagnetic showers (*e.g.*, e^- and γ) and only 10% due to hadronic showers (*e.g.*, *n, p*).[27]

As the energy of the incoming particle is transferred to the material, there are several damage mechanisms which can occur. Which reactions occur is a function of chemistry and the conditions of irradiation. These mechanisms are outlined below:

Radical Formation

When an uncharged species does not have the correct number of bonds, it is called a radical. These highly reactive species are missing an electron to complete their outer shells. Examples of radicals include •H and •CH_3 but also include long chain molecules with one site missing. These radicals may be frozen in at low temperatures and cause damage upon warmup. Radicals are formed by the reaction:

$$\mathbf{R} + \gamma \longrightarrow 2\,\mathbf{R}\bullet$$

Gas Evolution

Bonds between the main chain and small side groups like H, Cl, or CH_3, which are mobile within the matrix and can combine into stable molecules which are gaseous at room temperature. These molecules may not be mobile at low temperatures, but can combine and diffuse out at higher temperatures. These gasses often coalesce into bubbles and cause swelling.

Crosslinking

Sometimes, a radical will interact with a nearby chain. The two chains are then chemically linked. This tends to embrittle the material. Crosslinking occurs by:

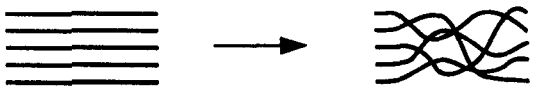

Chain Scission

When the bond broken by the radiation is a main chain bond and the chain is broken into two pieces, chain scission is said to have occurred. Chain scission tends to weaken the material. The reaction is:

Oxygen

The presence of oxygen can complicate the situation. The oxygen molecules can serve in a propagation reaction, such that several radicals are formed from the one created by the irradiation. The reaction is as follows:

Initiation $R\bullet + O_2 \longrightarrow ROO\bullet$

Propagation $ROO\bullet + R \longrightarrow ROOH + R\bullet$

$ROOH \longrightarrow RO\bullet + OH\bullet$ *or* $ROO\bullet + H\bullet$

These microscopic chemical changes in the molecules of the material induced by the radiation cause changes in the macroscopic properties of the bulk material. If one models a polymer as a knot of yarn or spaghetti on the microscopic level, the mechanism by which these changes occur is often easy to grasp. As an example, consider chain scission. According to the knot model, cutting the length of the strands results in fewer entanglements and less strength but higher elongation to break, which is in fact what happens to the bulk material. One may find it useful to consider putting several bulk properties into this model.

Consider electrical properties. As long as the energy in the bonds of the remaining links is greater than the energy liberated by an electron at the induced voltage traveling through the material, it will remain an insulator. Severe mechanical changes should be predicted after there are so few bonds remaining that the material is no longer an insulator. In fact, studies of electrical properties[1,13,21] have found that electrical property changes do in fact occur at similar or higher doses than mechanical property changes. One study[21] suggests that the application of a mechanical load is often the cause of electrical failure which would not otherwise have occurred. Dielectric loss changes have been found to be frequency dependent.[13] Crosslinking tends to decrease dielectric loss whereas chain scission tends to increase it.[13] It has been hypothesized[13] that this change is due to mobility of polar groups or ions to carry charge. Transient increases in conductivity under irradiation were measured and found to be dose rate dependent.[13] As magnets have empirically performed in these environments, it is thought that this effect is unimportant. Like electrical properties, thermal properties have been found[18] to not degrade with dose until after mechanical properties degrade.

Differences have been found[18,22,23] between *in situ* and *ex situ* effects of irradiation on creep properties. There was an increased rate of creep at higher dose rates.[18] The combination of stress and irradiation was found to be more damaging due to a synergistic effect. *In situ* testing was rejected for this study due to budget and schedule constraints.

The chemical reactions, like crosslinking, which cause damage to the materials after the deposition of energy due to radiation, can be expected (to first order approximation) to follow the Arrhenius relationship[15,24] and depend on temperature. Dose rate dependence is assumed to be due to the effects of oxygen, and little dose rate dependence is expected in an inert atmosphere.[15,24] Attempts have been made[24] to account for the temperature and dose rate effects. Because irradiation will take place in an inert atmosphere, dose rate was not considered to be a problem. Some studies[25] found a difference between room temperature and cryogenic irradiation, and others[17] did not. A high temperature anneal after irradiation was found[26] to result in increased damage due to activation of latent frozen-in radicals. It was therefore felt to be important to perform the tests at 4 K and warmup the samples after irradiation to simulate warmups in service.

It is also important to note that in a composite, the fiber/matrix interface bonds and halogen bonds are often damaged preferentially. As the fibers are much stronger than the resin, destroying the interface bond tends to reduce the impact of the fiber on the bulk properties. Halogenated polymers tend to release in organic acids (*e.g.*, HCl, HF, *etc.*) which can damage nearby components.[13]

3.0 METHODOLOGY

3.1 General Approach

This study was designed to simulate conditions in the Collider main ring and High Energy Booster (HEB) magnets as closely as possible. Materials expected to be used in the coldmass as end parts, insulation, or adhesives were exposed to a nominal dose of 10^9 rads, which is the design dose. Materials expected for use outside the coldmass for posts, the bus pulltrusion, or splice plates, were exposed to a nominal dose of 10^8 rads, the design dose for these parts. Ideally, one would like to irradiate to several levels to get a trend of properties with dose. Due to time and budget constraints this was not possible. Irradiations were performed with samples submerged in liquid helium. Heat transfer calculations described in Appendix A indicated that the maximum dose in the samples never rose above 20 K. The irradiated samples were shipped in liquid nitrogen and warmed up for one week prior to testing to simulate warmups in service. Mechanical testing was performed at 4 K.

3.2 Site Selection

The General Atomics (GA) site was selected after an extensive search. First, it was determined that an electron beam would be used. The choice of an electron beam was based on the fact that the majority of the spectrum is calculated to be electromagnetic showers.[27] Reactor irradiation was ruled out because a reactor spectrum has too many neutrons[27] and because of the higher dose rates available using electron accelerators. Data were collected on a variety of electron accelerators around the country and a review of this data for availability and cost of beamtime, experience with cryogens, beam energy and other parameters narrowed the search. Three sites were visited and sent a request for quote. The site was selected based on the evaluation of the quotes received.

3.3 Test Development

The tests performed on the materials in this study were selected based on review of previous research and examination of potential failure modes. For composites, resins, and filled systems, it has been found that shear strength tends to fall off before compressive or tensile strength.[1,10] Flexure is often used in radiation damage studies[3,10,16,17,22] and is recommended by the International Electrotechnical Commission (IEC)[15] for rigid materials. The flexure test was chosen for resins and filled systems for that reason. To ensure failure in shear for laminated composite samples, the short beam shear test was selected. The short beam shear test is an indirect test for interlaminar shear strength because when the interfacial shear strength exceeds the matrix shear strength, failure occurs in the matrix and the strength value reaches a plateau. For this reason, these values will be reported as Apparent Interlaminar Shear Strength (AISS). For resins and composites, weight, dimensional, warpage and color changes were observed as well. For films, tension is relatively easy, will simulate in use conditions, and is in accordance with IEC recommendations.[15] Lap shear was chosen for adhesives because peel strength requires a larger number of samples, is difficult to do at 4 K, and because shear is the expected failure mode. The difficulty of sample preparation led to the rejection of the adhesive laminate short beam shear test method that had been used at Brookhaven National Laboratory (BNL). The development of the lap shear test method as used in this study was done by George Darr at Composite Technologies Development (CTD) in consultation with the author. Figure 1 shows the sample configurations for each of these tests.

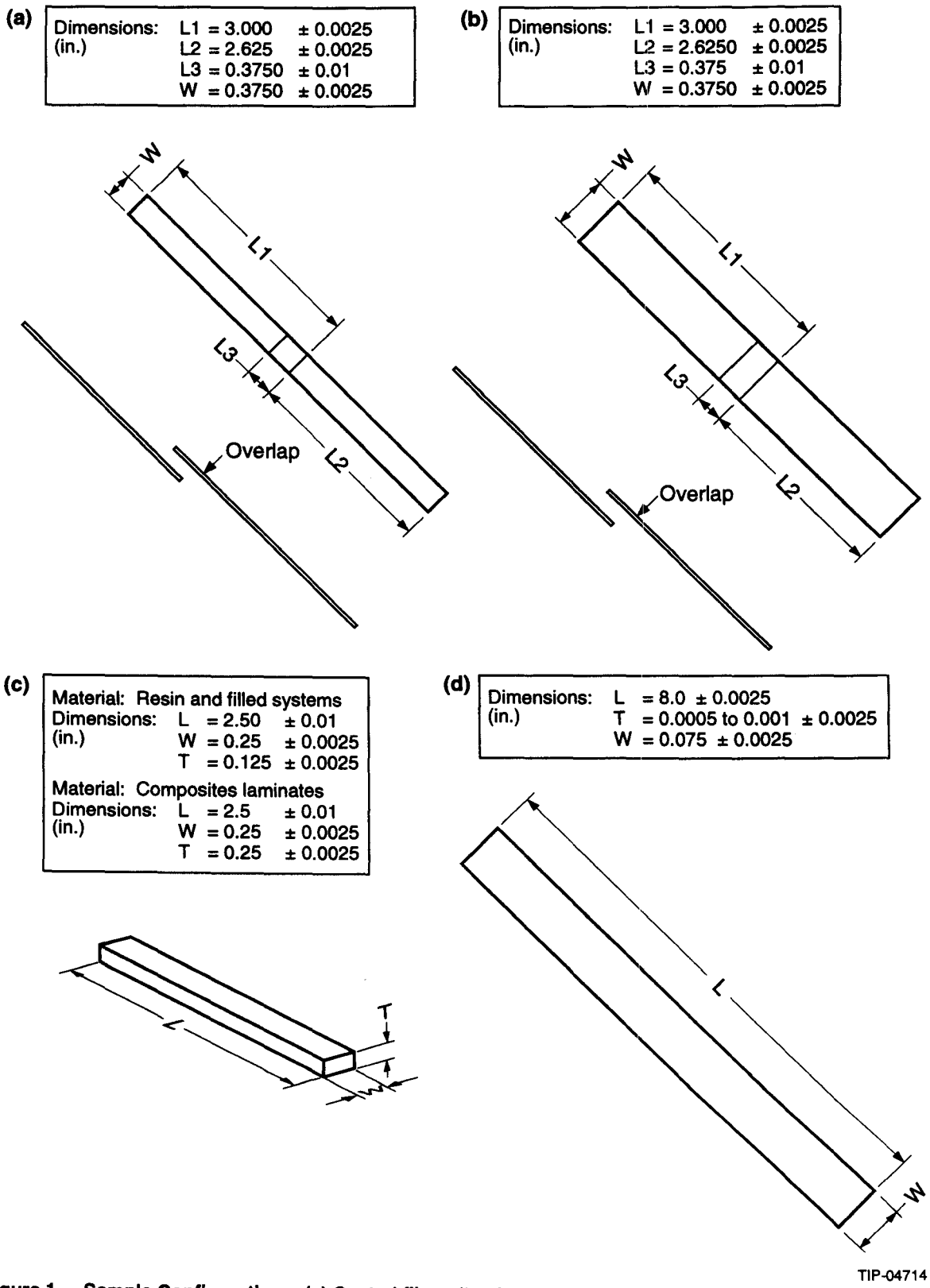

Figure 1. **Sample Configurations. (a) Coated film adhesive, 0.2–0.3 mils of B-staged adhesive were coated on one side of polyimide film and the samples were cured with the adhesive sides facing each other as per use in magnet. (b) Prepreg samples were cured as per use in magnet. (c) Composites, resins, and filled systems. (d) Film.**

3.4 Material Selection

Table 1 lists all materials irradiated in this program. Materials were selected by identifying candidates for specific uses in each program. For example, the Collider Quadrupole Magnet (CQM) material candidates selected by Siemens are:

Material	Application
Permaglass TE630	end parts
Isopreg E0315	prepreg
Permaglass ME730	splice plate
Kapton VN	insulation
Araldit AV1580 GB/hardener	putty/filler

TABLE 1. LIST OF MATERIALS.

Material	Vendor	Dose (rads)
Composites, Resins, and Filled Systems		
Spaulrad	Spaulding Composites	10^9
CTD101G	CTD	10^9
Cryorad	Allied Signal	10^8, 10^9
PEEK	Victrex	10^8, 10^9
VTEM1	UDD-FIM	10^8, 10^9
Ultem 2300	GE	10^8, 10^9
Vespel SP1	DuPont	10^9
Torlon 5030	Amoco	10^9
Isaryl 15X	Isonova	10^9
Ultem 6200	GE	10^8, 10^9
Envex 5630	Rodgers Corp.	10^8, 10^9
CP 1525	Creative Pulltrusions	10^8
CP 1625	Creative Pulltrusions	10^8
Araldit/hardener	Ciba-Geigy	10^9
TE 630	Permaglass	10^9
ME 730	Permaglass	10^9
Films		
Kapton H	DuPont	10^9
Kapton HA	DuPont	10^9
Kapton LT	DuPont	10^9
Kapton HN	DuPont	10^9
Kapton XMPI	DuPont	10^9
Apical NP	Allied Signal	10^9
Apical AV	Allied Signal	10^9

TABLE 1. LIST OF MATERIALS (Continued).

Material	Vendor	Dose (rads)
	Adhesives	
XMPI	DuPont	10^9
Modified XMPI	DuPont	10^9
CTD 105	CTD	10^9
Cryorad	Allied Signal	10^9
3P	Sheldahl	10^9
Modified 3P	Sheldahl	10^9
EX 1508	Bryte	10^9
5575-2	BASF	10^9
E 388D	BP Chemicals	10^9
EPO316	Isovolta	10^9
EP VP 1037/I	Isovolta	10^9

Some additional adhesives were selected on the basis of likelihood of survival based on chemistry. Because the adhesive samples were very thin, no additional irradiation costs were incurred by placing more samples in the dewar for irradiation. There was, therefore, a minimal cost to exposing additional samples. Many of these adhesives had been identified by Mr. Morena.[28]

3.5 Preparation

3.5.1 Samples

Samples were requested from material vendors to be processed as they would be used in the magnet. For instance, samples cut from injection molded plates were irradiated if the magnet part was to be formed by injection molding. Adhesive samples were cured as they would be in a magnet. Samples were marked on or near the ends for identification, weighed in groups, and measured in three places along the length in both thickness and height. All of this information was recorded on a traveler to accompany each group of samples to be used for comparison after irradiation. Many of the samples of resins, composites, and films were requested by John Morena for the BNL program and were left over, which allowed considerable time savings. All adhesive samples were fabricated for this test because the configuration of the BNL adhesive samples was different than the sample configuration for this study.

3.5.2 Irradiation Dewar

A dewar was built for this program. The design was done by Mike Tupper and revised in consultation with Jon Zbasnik and the author. The drawings were then submitted for construction. Figure 2 shows the dewar.

3.5.3 Dewar Alignment

The dewar was aligned to the beam by lifting the dewar onto a platform and adjusting the platform location. Coarse adjustment involved placing a piece of polycarbonate on the platform and irradiating the piece. The bubbling of the polycarbonate provided positive indication of beam location. The dewar window was placed as close behind the bubbled section as possible. The collimators were then placed upstream of the dewar. Fine adjustments were made by several iterations of placing radiochromic film on the dewar window, collimator openings, and on samples inside the dewar, reading the films after exposure, and moving the appropriate piece of equipment.

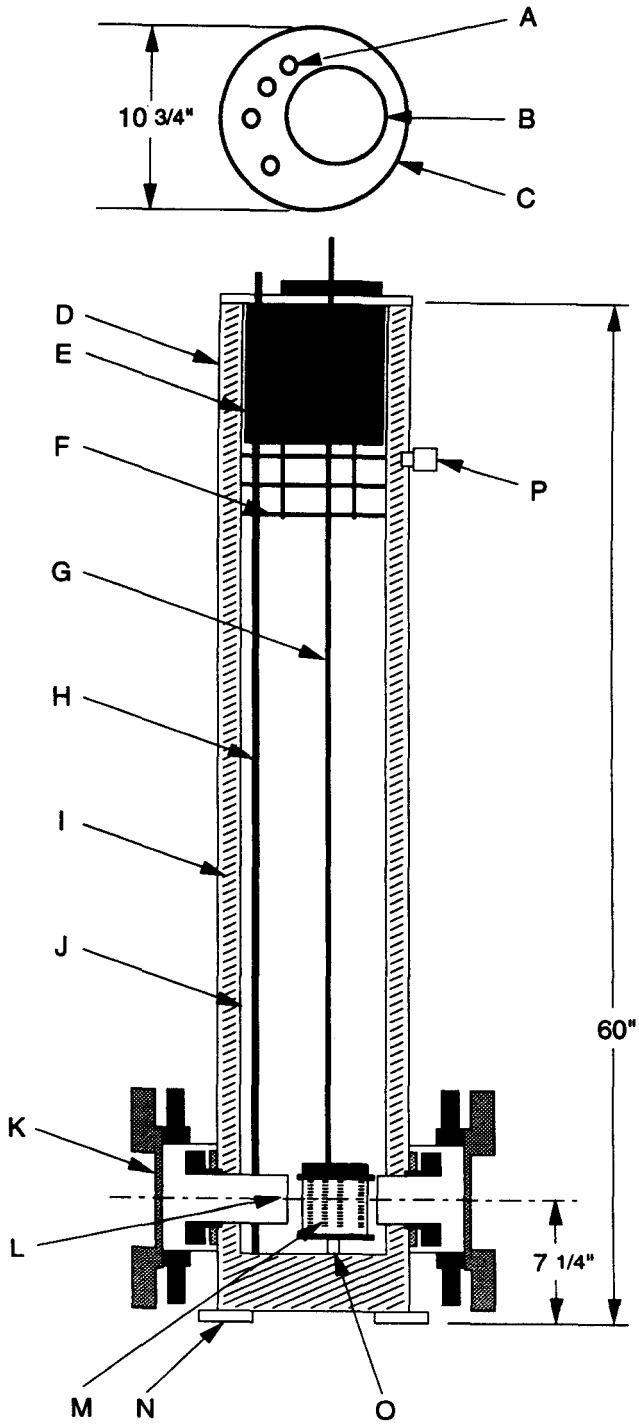

Key to dewar drawing

A Top plate penetrations
- Liquid helium fill
- Helium vent
- Liquid helium level sensor
- Additional instrumentation

B Specimen holder top plate
- phenolic

C Dewar top plate
- 304 SST

D Vacuum vessel
- 10" sch 10 304 SS

E Foam thermal insulation

F Aluminum thermal radiation shields

G Specimen holder support shaft

H Liquid helium level sensor

I Superinsulated vacuum space

J Helium vessel
- 8" OD x 0.64" wall 304 SS tube

K Vacuum vessel beam windows
- aluminum 6061, 0.1" thick

L Heilum vessel beam windows
- aluminum 6061, 0.40" thick

M Specimens in specimen holder

N Dewar support and mounting tabs

O Specimen holder locating pin

P Vacuum pump-out and relief valve

TIP-04715

Figure 2. Irradiation Dewar.

3.6 Irradiation

3.6.1 Setup

Figure 3 shows the equipment setup. The Linear Accelerator (Linac) port window, dewar windows, and collimators are all made of aluminum. The collimator holes are 1.375 in. square. Samples in the dewar were arranged in a 6 × 4 array with 1/16 inch between samples in the short direction and 1/10-inch spacing between samples in the long direction. Samples were suspended from the top of the sample holder with setscrews. The alignment of the system was crucial to the program to ensure a uniform dose to the samples. Several parameters affect the alignment of the samples inside the dewar, one of which is the tuning of the accelerator. As alignment is a lengthy process requiring several iterations of adjustments, it is preferable to avoid it. It took quite a while to work out the dewar support system and beam tuning so that measurements were repeatable. The Linac was not turned off after calibration runs until after the last experimental run to avoid the need to recalibrate after the beam was tuned.

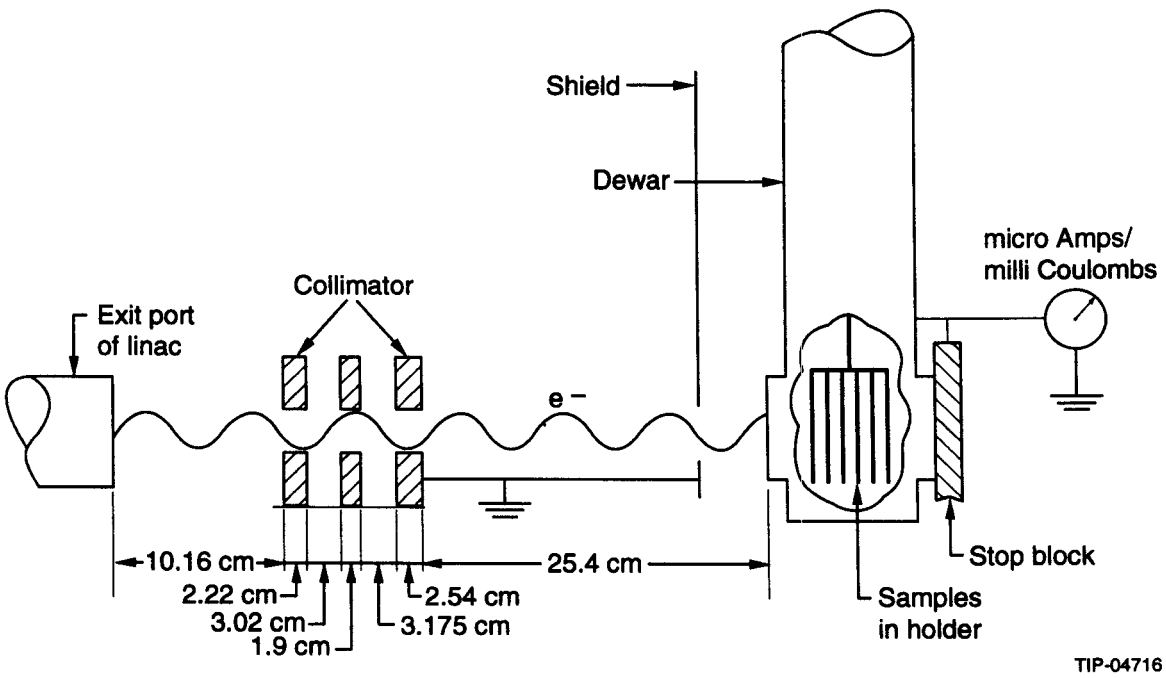

Figure 3. Irradiation Setup.

3.6.2 Procedure

Irradiations were performed according to the following procedure developed at General Atomics (GA) by the author as an adaptation of ASTM, E 1027, 1984.[29] All deviations from this standard are mentioned in this report. After ensuring there was a sufficient supply of liquid nitrogen, liquid helium, gaseous helium, and SF_6 (to insulate wave guides in the Linac) to complete the runs, dosimetry runs were performed. For film and adhesive sample dosimetry runs, four dummy runs were done at room temperature with a sample simulating the stack of films and adhesives. For resin and composite dosimetry runs, four full arrays of 24 dummy samples each were irradiated. Each dummy sample in a dosimetry run had radiochromic film on two sides opposite to each other. The radiochromic film was taped to the dummy samples, centered with respect to the length of the sample for resin and composite dummy runs, and several places along the length for film and adhesive dummy runs. The attaching tape did not cover the portion of the film which was to be read. If the tape came into contact with the portion of the film which was to be read, touched with bare hands, or exposed to direct light, that film was discarded. These filmed dummy samples were placed in the sample holder in the

same manner as real samples with the filmed surfaces perpendicular to the beam direction. The samples were placed in the room temperature dewar and irradiated on both sides to the desired number of milliCoulombs. The current and time integrated current were measured in realtime from the same signal by electrically isolating the dewar and providing only one path to ground through the meter. A piece of radiochromic film was placed in the front of the window before the irradiation of each side and exposed with the samples. The films were read, the film readings analyzed, and the correct number of milliCoulombs and irradiation rate in microAmps for the upcoming runs computed and reported. The details of these calculations can be found elsewhere in this report. A map of the type and sample number of each specimen and its location and orientation in the specimen holder was prepared for each run on the run log for later comparison to the dose distribution data. The dewar was then cooled by precooling with liquid nitrogen, purging the nitrogen with gaseous helium, and then transferring liquid helium into the dewar. For 10^9 rad runs LiF crystal, which had been reset and whose initial transmittance measurements had been taken, was placed in the front of the window in the same position the films were placed in the calibration runs. Samples were irradiated to the proper number of milliCoulombs on that side, the sample holder rotated 180° inside the dewar, the crystals replaced, and the other side irradiated similarly. The 180° rotation was performed to insure uniformity of dose. After completion of the irradiation, the specimens were stored in LN_2. The transfer of the samples from the sample holder to the storage dewar was done as quickly as possible, without allowing the samples to warm to room temperature. After the first irradiation run, subsequent runs were done in the same manner, except that calibration runs were not repeated. For all runs, the pulse rate was 30/sec, the duty cycle was 0.001, the irradiation time was 2 hours for 10^8 and 19 hours 10,^{9} the pulse peak energy was 18–20 MeV. The observed boil-off rate was 1.8 litres/Mrad.

3.6.3 Calculations

Given the need to keep the temperature in the center of the sample at or below 20 K, the heat input was kept below 1 Watt per sample. The 1 Watt/sample requirement was calculated by Charlie Corbett. His calculations and results are included in Appendix A. The number of μAmps required to deliver 1 Watt/sample was calculated in a conservative manner. First, it is known from dose-versus-location studies with radiochromic film that the height of the intense portion of the beam is approximately 1 inch. The weight of the irradiated part of a dense sample is approximately 1.8 grams. Recall that a Watt is defined as a Joule/second and a rad is defined as 10^{-2} Joules/kg. From this it is determined that the highest dose rate should be 5.55×10^4 Rad/sec. The slope of the calibration curve of Mrads-per-milliCoulomb is then used to find the current which will achieve this dose rate for the first samples in the beam path. The dose rate to subsequent samples will be lower. Given the fact that the samples are rotated halfway through the procedure, the average dose rate for all the samples over the entire run is approximately 2×10^4 Rad/sec.

The dose distribution was calculated by N. Mokhov using a Mars12 Monte Carlo simulation using the actual sample configuration, beam distribution at the window of the dewar, and assuming a uniform energy distribution of 20 MeV. The calculation was done for air and liquid helium in the dewar. There is no significant difference in dose distribution between air and liquid helium according to Dr. Mokhov.

3.6.4 Problems

Several minor problems were encountered in this program. Although sample identification was supposed to be unique, the number 44 was very popular. This should not have been a problem because there were no repeated serial numbers in an individual run and the samples for an individual run were stored together. Unfortunately, the dewar was tipped during transport and the duplicates were mixed together. Most of these duplicates could be identified easily by color, but two samples were discarded. Fortunately, both of these samples were of materials for which there were more than five irradiated samples. For the first 10^8 rad run, half of the samples fell out of the sample holder, necessitating another 10^8 rad run. For the first 10^8 rad run there was no external dosimetry. In the second 10^8 rad run, the films that were to be used for external

dosimetry were not changed during the run and were badly saturated. The dosimetry on the 10^8 rad runs is therefore very approximate. In one instance there was a shortage of liquid helium and the helium in the dewar boiled off to a level thought to be below that of the samples. Because the situation was recognized, the samples were not being irradiated until helium arrived. The situation was analyzed and it is believed that the samples were still below 20 K because they were surrounded by gaseous helium at 4 K.

3.7 Dosimetry

The measurement of dose was the most difficult part of this experiment. After long search, it was determined that there is no known easily calibrated method to measure to 10^9 rad at 4 K either in realtime or in post irradiation analysis. In fact, it was difficult to locate a system which would measure to 10^9 rad even at room temperature as articles about dosimetry at "very large absorbed doses" often mean[30,31] 10^8 rad. It was determined that nylon based FWT-60 radiochromic films would be used for dose distribution characterization and verification of beam centering. The 510 nm wave length was chosen for use because it is good to a higher dose level and is less humidity sensitive.[32] Use of a Faraday cup and recreating the 4 K irradiation configuration at room temperature has been used as a method of dosimetry with good results,[33] but an actual on-line measurement, or positive post irradiation indication of dose is preferable. The method chosen for the post irradiation dose measurement was spectrophotometry of LiF chips. LiF chips are widely used for dosimetry as thermoluminescent dosimeters. Unfortunately, the thermoluminescent effect saturates well below 10^9 rad. The use of optical absorption bands for dose measurements has been well documented[33–37] and the advantages of their use described.[38] Each crystal must be calibrated separately.[36,37] Although these crystals have been irradiated at cryogenic temperatures,[33,34] it was not possible to have them calibrated at 4 K. Optical absorbency readings were taken at $\lambda = 785$ nm. Both the LiF crystals and the radiochromic film were calibrated at National Institute of Standards and Technology (NIST). The spectrophotometer readings for the same samples were also compared for the GA spectrophotometer and the NIST spectrophotometer.

After a long characterization process, several conclusions were made. First of all, it was assumed that the dose distribution was the same at room temperature and 4 K. It was found that the dose distribution at room temperature measured as described earlier in the radiation procedure section with radiochromic film batch 3E2 measured on a Far West reader was repeatable. If one arranges the materials according to Figure 4, the average dose of each material is within 5% of the average dose over all the samples in the dewar, meaning that although the sample-to-sample variation is around 30%, the material-to-material variation in a particular exposure is very small. Because the sample arrangement allowed for 24 samples of 0.25 × 0.25 inches and five samples per material were required, eight 0.25 in. × 0.125 in. samples were placed in the remaining four sample slots (labeled 5 in Figure 4). In some cases, two 0.25 in. × 0.125 in. samples were placed back to back instead of one 0.25 × 0.25 inch sample. The position of each sample was recorded on the run logs. If one placed film in the bottom of the dewar window, the front film reading could be correlated to the average dose to the samples inside the dewar. The slope of average sample dose versus dose outside the window changed with tune but was very consistent for a specific tune. Figure 5 is a sample dose vs. window dose curve. The average dose of the samples in the dewar was plotted vs. milliCoulombs, which were measured during the experiment. As long as the beam was not shut off or retuned, the plot of dose vs. mC was very close to a straight line as can be seen in Figure 6. In addition, each 10^9 rad exposure contained five Torlon 5030 samples as a cross check between exposures. The calculated dose for the materials in run 2, Cryorad, Spaulrad, Vespel, and Isaryl was 1.1×10^9 rad. The calculated dose for the materials in run 3, ME730, VTEM2, CTD101G, Ultem 2300, and Ultem 6200 was 0.96×10^9 rad. The calculated dose for materials in run 4, Envex, Aryldite, TE630, and PEEK was 0.83×10^9 rad. The calculated dose for all films and adhesives was 3.7×10^9 rad. The dose to the film and adhesive samples was higher due to the fact that the system was not as well characterized as the resin and composite configurations.

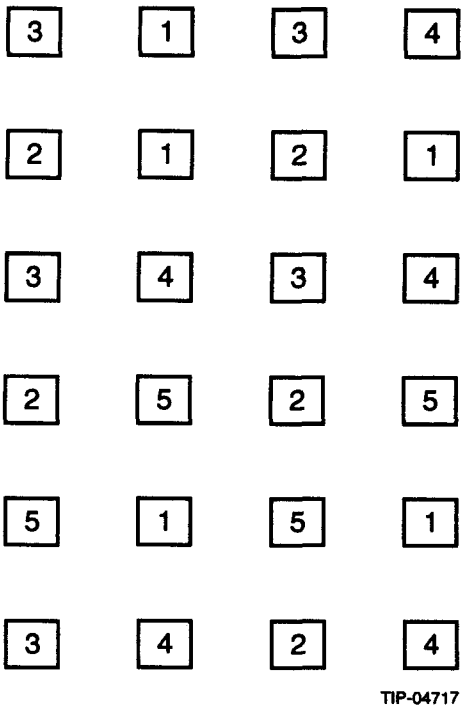

Figure 4. Sample Arrangement in Dewar. Numbers correspond to material type (*e.g.*, Torlon).

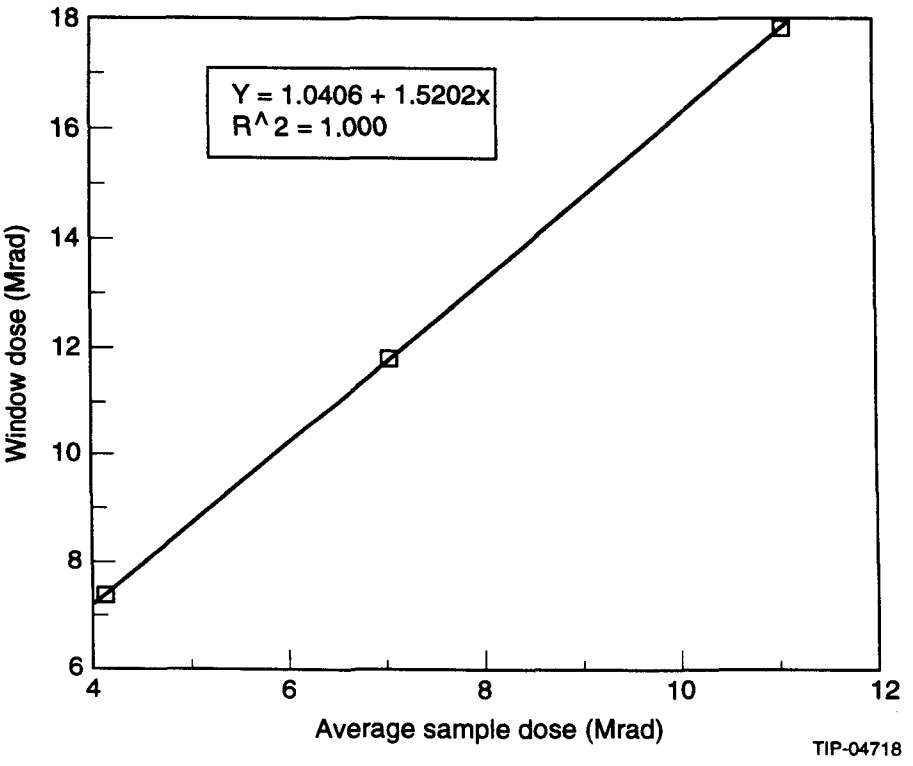

Figure 5. Sample Dose vs. Window Dose; Window to Sample Calibration (8 Feb.).

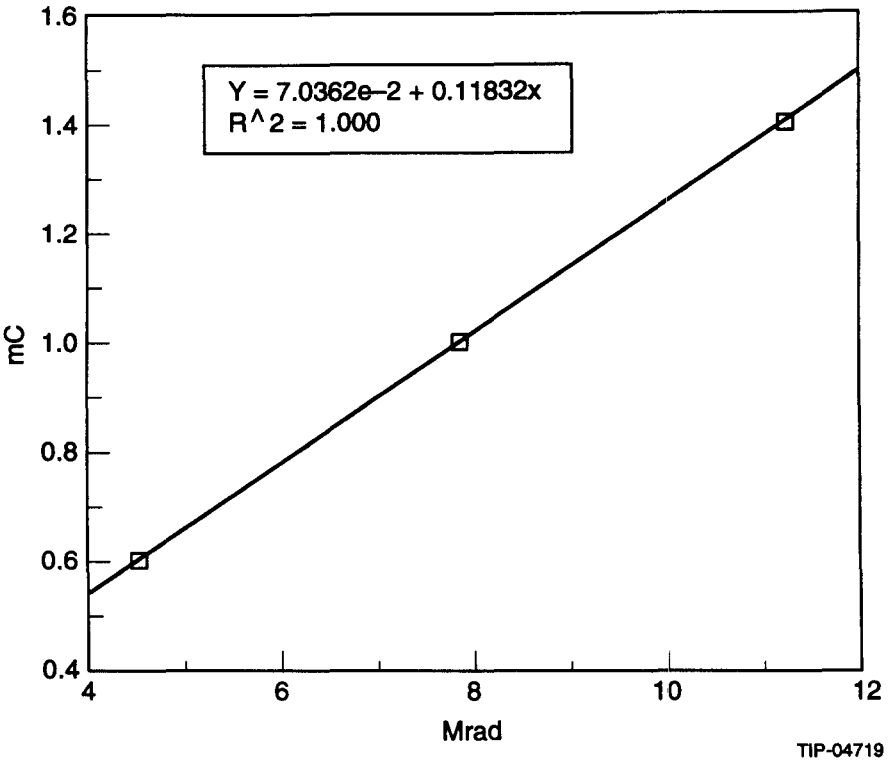

Figure 6. Average Sample vs. milliCoulombs; milliCoulomb to Sample Calibration (Jan. 28).

3.8 Testing

All irradiated samples were shipped in a special dewar filled with liquid nitrogen to CTD for testing. Approximately 30 resin and composite specimens or 20 film or adhesive specimens were removed per day until all samples were removed. The samples were then kept in an environmental chamber with a constant temperature of 27°C for one week. The environment was controlled by a Omega CN9000A controller with feedback from a type T thermocouple and heat input with tape. Humidity was monitored daily using an OMEGA RH70 and was maintained by placing a pan of water in the bottom of the chamber. The humidity was between 55% and 65% RH throughout the experiment. The one week warmup is to simulate the warmups of the magnets that are expected in service. The magnets will be warm for more than a week in service, but one week was felt to be sufficient to allow for escape of gasses and diffusion of free radicals and short enough to not cause delay to the program. After the seven day warmup, the samples were tested. Control samples had been tested previously in many cases and had not been thermal cycled or held in the environmental chamber. As a result, the control samples that were tested for this report were treated similarly to the previous control samples. Resin and composite materials were tested for warpage, color change, weight change, swelling, and mechanical properties. Films and adhesives were tested for mechanical properties. Occasionally, not all tests scheduled for a particular day could be completed. In those cases, the remaining samples were put back in liquid nitrogen and kept there until they could be tested.

All preliminary observations were made according to the following scale:

Severe	Severe Damage	4
Significant	Casual Glance	3
Moderate	2nd Look	2
Slight	Compare to Standard	1
None	Not Changed	n/c

3.8.1 Warpage

Samples were inspected for warpage by comparing sample sides to a straight edge. Control and irradiated samples were inspected for warpage and the results compared. All control samples were either not warped or slightly warped. Some samples were slightly warped for both irradiated and unirradiated, but the irradiated samples were more warped than the control. These materials are reported as very slightly warped; results of these observations are noted in Table 2.

3.8.2 Color Change

Control samples of each resin and composite material were placed next to irradiated samples for each run separately. Color changes were noted for each direction for materials for which there was a difference. In all such cases, the sawed edges were discolored less than the smooth edges. Only one material, Vespel, got lighter. In all other cases, irradiation induced darkening of the materials. The results are reported according to a scale analogous to the warpage scale in Table 2.

3.8.3 Weight Change

Samples or groups of samples were weighted to at least the nearest 0.1 gram, and in most cases to the nearest 0.0001 gram. These samples or groups were weighed again after irradiation. There was no change in weight for any materials except for Ultem 6200 which gained almost exactly 20%. It is thought that the weight reported for five samples prior to irradiation was actually for four samples. The weight of a leftover unirradiated Ultem 6200 sample was consistent with this hypothesis.

3.8.4 Dimensional Change

All samples were measured before and after irradiation to check for swelling. No measurable swelling was observed.

3.8.5 Mechanical Testing

All mechanical tests were performed using a 110 kip MTS test system with a 22 kip load cell, computer data acquisition, a 20 litre dewar, and a type T thermocouple with ice point. The short beam shear and flexure tests were based on ASTM D2344-84. After alignment of the fixture and setting the appropriate span ratio, 4 for flexure, the sample was centered on the 1/8" lower pins and a preload of around 20 lbs applied to prevent the sample from floating off the test fixture. The sample was then covered with a shield to contain the parts and to facilitate sample retrieval after testing. Initially, the fixture and sample were first cooled with LN_2. After boiling stopped, the nitrogen was emptied and the dewar filled with liquid helium. The temperature was monitored about an inch above the sample and displacement drift due to thermal contraction of the actuator rod was monitored also to ensure that the temperature had stabilized at 4 K before beginning the test. The test was run in stroke control at a rate of 0.5 in./min. Upon completion of the test, the dewar was lowered, the actuator lifted, the sample removed, and another sample placed in the fixture. Successive samples were

cooled with only helium because the majority of the thermal mass, the load cage and sample fixture, were already cold.

The tensile specimens were mounted in pressure plate grips with raised pressure ridges, the gage length measured, and precooled in liquid nitrogen. The specimen grips were mounted to the testing machine with pins. The samples were cooled to 4 K under a preload of approximately 5 lbs. Testing was performed at 0.5 in./min. Cryogenics procedures were similar to those described above.

The lap shear tests required preparation of the samples before testing. The as-received samples were measured with an optical microscope with traveling stage and digital micrometer. The samples were glued to 0.032 inch thick 6061-T6 Aluminum backing plates using CTD 620NR cured at 120°F for 5 hours. Two extensometers were attached to the sample, one on each side. The samples were mounted the same method just described for tensile specimens. The preload during cool down for adhesive specimens was approximately 25 lbs. Testing was performed at 0.05 in./min.

4.0 RESULTS

4.1 Preliminary Observations

The results presented herein (Table 2) are from observations described previously under the heading of testing methodology.

TABLE 2. OBSERVATIONS.

Composites				
Material	**Warpage**		**Color**	
	10^8	10^9	10^8	10^9
Spaulrad	–	n/c	–	3
ME 730	–	n/c	–	3*
CP 1625	n/c	–	n/c	–
CP 1525	1	–	1	–
Cryorad	n/c	n/c	2	3
TE 630	–	1	–	3
VTEM 2	n/c	n/c	2	3
Resins and Filled Systems				
Ultem 2300	n/c	2	n/c	2
Ultem 6200	n/c	n/c	2	3
PEEK	1	1	n/c	n/c
CTD 101G	–	n/c	–	2
Vespel SP1	–	n/c	–	1
Araldit	–	1	–	1
Envex 5620	1	2	n/c	n/c
Torlon 5030	–	n/c	–	n/c
Isaryl 15X	–	n/c	–	4

* Delaminated during irradiation along edges

4.2 Mechanical Testing

The results presented herein are from observations described previously under the heading of testing methodology. Table 3 contains a listing of the unirradiated properties of the materials. Also listed is the percent change in the mean of the property with respect to the control (unirradiated) samples. These results were subjected to statistical ANOVA analysis to determine if the change in mean was significant (90% confidence) and only significant results are reported. Outlying results were eliminated in accordance with ASTM E 178-80, except for adhesives where failure mechanisms were examined and some additional samples were also eliminated on that basis.

The results presented herein are from observations described previously under the heading of testing methodology. Table 3 contains a listing of the mean values of the unirradiated properties of the materials. Also listed are the means of the properties measured at the exposed levels of radiation where these properties were significantly different from the control properties.

The results reported for the mechanical tests were subject to various statistical analysis procedures. Each observation was assumed to be reported without error in lieu of repeatability and reproducibility results for the mechanical test methods. Sets of observations for each of the materials were tested for outliers using exploratory data analysis techniques (box plots) and various analytic methods (t-test, Tietjen-Moore test) described in ASTM E178-80.[39] Adhesives were also examined visually to evaluate the cause of failure. Some adhesive samples were eliminated as a result of this examination. One Way Analysis of Variance (ANOVA) was used to test for significant changes in the mean response due to radiation effects. Typically, significance was defined at the 95% confidence level. For cases in which more than one radiation level was used, significant ANOVA results were subject to pairwise comparison techniques.

If there was no statistically significant difference between the 10^8 rad and 10^9 rad results, the average 10^8 rad result was reported and no change (n.c.) recorded for 10^9 rad. In other cases, there was no difference between the control and 10^8 rad, but there was a difference at 10^9 rad. In those cases, no change was reported at 10^8 rad and the average 10^9 rad result was reported. In cases where there was a difference between 10^8 rad and 10^9 rad, both results are reported. All dose levels in Table 3 are nominal dose. For exact doses refer to the section on dosimetry. Raw data is provided in Appendix B.

TABLE 3. RESULTS OF MECHANICAL TESTS.

COMPOSITES

Material	AISS (ksi)			MODULUS (Msi)			DISPL @ FAIL (in.)		
	0	10^8	10^9	0	10^8	10^9	0	10^8	10^9
Spaulrad	9.62	–	10.3	3.415	–	n.c.	0.042	–	n.c.
ME 730	12.0	–	n.c.	2.04	–	2.34	0.034	–	0.031
CP 1625	5.54	n.c.	–	2.01	2.49	–	0.030	0.028	–
CP 1525	4.36	n.c.	–	1.71	2.06	–	0.030	n.c.	–
Cryorad P	4.02	4.60	n.c.	2.41	2.66	n.c.	0.044	n.c.	n.c.
TE 630	13.6	–	n.c.	3.74	–	n.c.	0.048	–	n.c.
VTEM 2	9.49	n.c.	n.c.	2.55	3.24	n.c.	0.054	n.c.	n.c.

RESINS AND FILLED SYSTEMS

Material	STRENGTH (ksi)			MODULUS (Msi)			DISP @ FAIL (in.)		
	0	10^8	10^9	0	10^8	10^9	0	10^8	10^9
Ultem 2300	61.9	n.c.	n.c.	1.20	1.28	n.c.	0.016	n.c.	n.c.
Ultem 6200	32.7	n.c.	49.3	0.796	0.853	1.02	0.013	n.c.	0.016
PEEK	59.0	62.7	n.c.	1.09	1.34	n.c.	0.016	n.c.	0.015
CTD 101G	33.5	–	n.c.	1.98	–	2.08	0.007	–	0.004
Vespel SPI	26.7	–	21.8	0.64	–	0.68	0.026	–	0.021
Araldit	21.6	–	n.c.	2.40	–	2.08	0.006	–	n.c.
Envex 5630	40.3	57.14	n.c.	1.04	n.c.	n.c.	0.025	0.032	n.c.
Torlon 5030	62.3	–	58.1	1.15	–	1.26	0.035	–	0.030
Isaryl 15X	45.0	–	48.4	0.722	–	0.816	0.021	–	0.019

ADHESIVES

Material	STRENGTH (ksi)		Material	STRENGTH (ksi)	
	0	10^9		0	10^9
Cryorad	1.15	n.c.	CTD 105	1.88	n.c.
EX1508	1.63	1.81	V388/D	2.37	1.78
m3P/LT	1.33	n.c.	CI/RCI	1.64	n.c
m3P/NP	2.65	1.88	RCI/RCI	1.44	n.c.
m3P/VN*	2.16	–	XCI/XRCI	1.59	n.c.
5575-2/1	2.22	1.83	EPVP1037	2.07	n.c.
5575-2/2	2.03	1.69	EP0316	1.03	n.c.

FILMS

Material	STRENGTH (ksi)		MODULUS (Msi)		STRAIN	
	0	10^9	0	10^9	0	10^9
Kapton HA	50.2	44.2	1.30	0.84	0.0662	0.0720
Kapton HN	74.1	42.1	1.75	1.00	0.0572	n.c.
Kapton H	60.1	52.5	1.66	1.03	0.06425	n.c
Kapton LT	34.7	n.c.	1.03	n.c.	0.05475	n.c.
Apical AV	73.8	51.0	1.82	0.968	0.0978	n.c.
Apical NP	67.5	59.8	1.87	1.37	0.0693	0.0584

5.0 DISCUSSION

The materials selected for this study were selected, in part, because they were expected to survive the radiation doses specified for their application. In fact, most materials performed very well.

5.1 Structural Composites

The two Creative Pulltrusions materials, CP1525 and CP1625, were intended for use in the bus assembly. They were only expected to be exposed to 10^8 rads and were, therefore, exposed accordingly in this study. The bus application structural requirements are minimal and the material is expected to do little more than support its own weight.

The other structural composites were considered for use as end parts. The structural and radiation requirements for end parts are much more demanding than for the bus assembly. Both Cryorad P and VTEM2 showed an increase in modulus after 10^8 rads, but no further change to 10^9 rads. Cryorad P additionally showed an increase in strength at 10^8 rads. ME 730 showed an increase in modulus at 10^9 rads and decreased displacement at failure. Spaulrad showed only increased strength to be significantly different. This behavior is characteristic of increased crosslinking under irradiation. First modulus increases are often accompanied by an increase in strength an/or decrease in displacement at failure. Then, with increasing dose, there is a plateau region where properties are relatively constant with dose. After the plateau region, there comes a point where properties begin to fall off rapidly with dose (the so called "cliff"). It can be reasonably assumed that none of these materials have reached the "edge of the cliff" at the exposed doses.

5.2 Resins and Filled Systems

The resins and filled systems were intended for use mainly as end parts, posts, or the bus assembly. One material, Araldite, was intended as a filler material. PEEK showed some increased cross linking with a plateau at 10^8 rads. CTD101G embrittled only very slightly at 10^9 rads. Vespel had an increase in modulus and decrease in displacement to failure indicating crosslinking, but it also lost strength. This may be indicative of conflicting mechanisms (cross linking and chain scission) indicating that the material may be close to property drop off with dose. Araldite (green putty) suffered only a slight (13%) decrease in modulus. This was surprising based on the fact that this material has a lower aromaticity than many other epoxies. Torlon had an increase in modulus and a decrease in displacement to failure with no change in strength upon irradiation, indicating embrittlement. Torlon 5030 was exposed in all three batches to 10^9 rad. This was done as a cross check with the dosimetry. There was no difference between the three batches of Torlon which is consistent with the dosimetry readings. Isaryl exhibited all three signs of embrittlement, increased strength and modulus, and decreased displacement to failure. Envex exhibited increased strength and displacement to failure with a plateau at 10^8 rads. Ultem 2300 had an increase in modulus at 10^8 rads and a plateau at 10^9 rads. Ultem 6200 had an additional increase in modulus at 10^9 rads and an increase in other properties at 10^9 rads as well. Unfortunately, the difference in the glass content between the two grades makes comparison of the resins difficult. Based on these results, however Ultem 2300 would be preferred due to the plateau effect over Ultem 6200. Ultem 2300 is also easier to process and cheaper than Ultem 6200.

5.3 Adhesives

In addition to strength measurements, all adhesive samples were examined with an optical microscope after failure for determination of failure morphology/mechanism. All adhesives were either unchanged or had reduced strength after irradiation except for EX1508, which gained strength. Prepregs were more prone to change due to radiation than coated films. EX1508 failures were all brittle and notch-sensitive. There was also cracking in the tab region. The European prepregs, EP VP 1037 and EP 0316, did not change strength, but the failure before irradiation in EP VP 1037 was along the lap joint, whereas afterwards failure occurred along the lap/tab interface. For EP 0316 all failures were along the bond in a clean break. There were a few experimental difficulties with 5575/2. There were two panels of nominally identical samples tested. A few of

the control samples were tested with only tabs along the grip section allowing a bending moment to be introduced along the bond area. The analysis of the data after those samples were eliminated showed a difference between the two panels tested prior to irradiation, but not after. This may be due to the reduced sample size of the before irradiation groups. If both panels of 5575/2 are analyzed together, there is still a significant strength reduction due to radiation. V388D lost strength, and the failure mode became less brittle. Before radiation, the failure was along the lap edge perpendicular to the bond. After irradiation, initiation of the failure was parallel to the joint, significant areas of debonding were found, and tearing of the fibers in the tab area were found.

The coated film adhesives degraded less than the prepregs. Neither Cryorad nor CTD105 were significantly changed by irradiation. Both were mostly brittle, notch-sensitive failures, with Cryorad becoming less brittle after irradiation. The CI/RCI system and its low-temperature cure substitute XCI/XRCI were both also unchanged. The CI/RCI failures were mostly along the lap. The XCI/XRCI failures were mostly notch-sensitive and perpendicular to the joint before irradiation, and more ductile after irradiation. The RCI/RCI bond was also less brittle after irradiation and its strength was also unchanged. The RCI/RCI bond had a lower initial strength value than the CI/RCI bond. This is because the bond of the adhesive to the substrate film affects the strength the bond as well as the bond of the adhesive to itself. This phenomenon is better illustrated by the family of modified 3P adhesives tested. The three materials, all cured to the same cycle, were modified 3P on Kapton LT, modified 3P on Apical NP, and a no MEK version of modified 3P on Kapton VN. The control strength varied with substrate film. The samples backed with Apical NP film had the highest strength before irradiation and had the most ductile failure before irradiation. After irradiation, these samples were slightly embrittled and more notch-sensitive. The samples backed with Kapton LT had the lowest strength before irradiation, but did not change strength with irradiation. These samples did change failure morphology with radiation. The control samples tended to fail perpendicular to the joint and were somewhat notch-sensitive, whereas the irradiated samples failed parallel to the joint. The no MEK version also did not change strength with irradiation but was slightly embrittled with radiation.

5.4 Films

Recall that the actual dose received by the films was 3.7×10^9 rads. There was strength degradation of up to 43%. These results compare well with previously published data,[1–6] which show that the strength of polyimide films drop off with dose sharply after approximately 3×10^9 rads. Because the specification calls for the materials to withstand only 10^9 rads, this should not be a concern. These materials were tested for the sake of completeness as their behavior in a radiation environment is already well understood.

Kapton LT is an alumina filled film. Because the alumina will not degrade significantly until much higher doses, it was expected that the LT film would be more radiation resistant. This was in fact the case.

The Kapton H and HN as well as Apical AV, which are chemically virtually equivalent, suffered loss in strength and modulus. This is the expected result due to chain scission. Note that all are semicrystalline and that accounts for the lack of corresponding increase in strain to failure for these films. The Kapton HA, which is also chemically equivalent but amorphous, did show an increase in strain to failure. Apical NP, which is a block copolymer with a rigid phase, which can be thought of as equivalent to a high degree of crystallinity, actually showed a decrease in strain to failure.

6.0 FUTURE WORK

Future work has been planned in consultation with the subcontractors. The current plans are as follows:

- CDM—flexure tests are to be performed on Lexan 4701 and Noryl N300 at 10^7, 3×10^7, and 10^8 rads as per procedures presented herein. These materials are under consideration for use in the bus assembly.

- HQM—adhesive CTD105, prepreg Hexcel F185, and composites Hexcel F650, Hexcel F655, and G10. All tests to 10^9 rads and to be tested as per procedures presented herein.
- CQM—composites CTD101A, Permali TP 700, Vetroninte 64.140, and a specific type of Cryorad compound. All tests to 10^9 rads and to be tested as per procedures presented herein. In addition, compression tests are to be performed in both warp and weft directions on the composites. Dielectric tests are to be performed on the same films tested herein in tension.
- Our in-house program for G11CR, PR500, a specific epoxy used as an assembly aid, Kevlar yarn, a new cure cycle of modified 3P, 5250-A adhesive, and Hexcel F655 as a prepreg (not as a composite). This request is for all in house programs and reflects the needs of several types of magnets. These materials are to be tested as per procedures presented herein.

ACKNOWLEDGMENTS

Because I find myself unable to sort the people who contributed to this project in order of the importance of their contributions, I will list them roughly in the chronological order in which their contributions were made. I want to thank Jon Zbasnik for giving me the opportunity to do this experiment and encouraging me when difficulties arose. I also would like to thank John Morena for material recommendation and sample procurement and Steve Bastian for sample preparation help. Several calculations were performed by Nicolai Mokhov and Charlie Corbett which were necessary to this report. I must thank Naseem Munshi, Mike Tupper, Dick Reed and Jeorge Darr at Composite Technologies Development (CTD) for working to develop the test methods and testing the samples. Bill McLaughlin at the National Institute of Standards and Technology (NIST) must be thanked, because without the benefit of his years of experience in the field of dosimetry and his willingness to provide help despite the many other demands on his time, this study would have been finished much later and been less thorough. Jay Jayakumar must be thanked for his efforts despite the difficulty he must have had having come into this project in the middle. Thanks are also in order to the Linac crew at General Atomics (GA) for their hard work and long hours on this job and to Annette Greenwood at GA for reading the LiF crystals, keeping track of the data, and her willingness and ability to help with miscellaneous lab services and equipment. Last, but not least, I must thank Doug Pollock for performing the statistical analysis.

REFERENCES

1. W. Maurer, "Neutron and Gamma Irradiation Effects on Organic Insulating Materials for Fusion Magnets," Institute of Technical Physics **3974**, ISSN: 0303-4003 (October 1985).
2. K. Abe, C. Logan, K. Saneyoshi, and F. W. Clinard, Jr., "Irradiation Effects in Kapton Polymide Film from 14 MeV Neutrons and Cobalt-60 Gamma Rays," Conference: Influence of Radiation on Material Properties: ASTM 13th International Symposium (Part II), ASTM STP-956, (ASTM, Seattle, WA, Jan. 1986), pp. 669–681.
3. C. J. Long, R. H. Kenohan, and R. R. Coltman, Jr., Author Affiliation: Oak Ridge National Lab., "Radiation Effects on Insulators for Superconducting Magnets," Non-Metallic Materials and Composites at Low Temperatures, Munich, West Germany, July 10–11, 1978, (Plenum Press, NY, 1979), pp. 141–53.
4. R. P. Reed and N. Munshi, "Effects of Irradiation on Selected SSC Magnet Insulators: A Review," Composite Technology Development, Inc., Boulder, Colorado, Sub-contract: SSC-92B-09316.
5. T. Sasuga, N. Hayakawa, K. Yoshida and M. Hayiwara, "Degradation in Tensile Properties of Aromatic Polymers by Electron Beam Irradiation," *Polymer*, Vol. **26**, No. **7**, July 1985, pp. 1039–45.
6. H. Yamaoka and K. Miyata; Author Affiliation: Res. Reactor Inst., Kyoto University, Osaka, Japan, "Radiation Effects on Organic Insulator Films at Low Temperature," *Journal of Nuclear Materials*, Vol. **133–134**, 1985, pp. 788–90.
7. S. Takamura and T. Kato; Author Affiliation: Japan Atomic Energy Res. Inst., Tokai-mura, Ibaraki-ken, Japan, "Effects of Low Temperature Irradiation on the Mechanical Strengths of Organic Insulators for Superconducting Magnets," *Cryogenics,* Vol. **20**, No. **8**, August 1980, pp. 441–4.
8. T. J. McManamy, G. Kanemoto, and P. Snook; Author Affiliation: Oak Ridge National Lab., "Insulation Irradiation Test Programme for the Compact Ignition Tokamak," *Cryogenics*, Vol. **31**, No. **4**, April 1991, pp. 277–81.
9. J. R. Benzinger, "Development of 3-D Composites," *Applications of Cryogenic Technology,* J. Patrick Kelly, ed. (Plenum Press, NY, Vol. **10**, 1991), pp. 197–206.
10. R. R. Coltman and C. E. Klabunde; Author Affiliation: Solid State Div., Oak Ridge National Lab., Oak Ridge, "The Strengths of G10CR and G11CR Epoxies After Irradiation at 5 K by Gamma Rays," *Journal of Nuclear Materials*, Vol. **113**, No. 2–3, Jan. 1983, pp. 268–72.
11. Manufacturer Supplied Data, Technische Innovationen, Ges.m.b.H., AR2355 Weiner Neudorf, Austria.
12. L. English, "How High Energy Radiation Effects Polymers," *Material Engineering,* Vol. **103**, No. **5**, May 1986, pp. 41–44.
13. V. J. Linnenbom, "The Effects of Radiation on Materials, Part 3 – Radiation Damage Insulating Mechanisms Insulating Materials," *Insulation,* Vol. **6**, March 1960, pp. 11–15.
14. N. Munshi, Composite Technology Development, Inc., Boulder, Colorado, U.S.A., "Superconducting Magnet Insulators: Radiation-Induced Damage and Effects," *Supercollider 3,* Edited by J. Nonte (Plenum Press, NY, 1991), pp. 107–115.

15. "Guide for Determining the Effects of Ionizing Radiation on Insulating Materials Part 2: Procedures for Irradiation and Test," Second Edition, Bureau of International Electrotechnical Commission, IEC 544, PT 2 (1991).

16. S. Egusa; Author Affiliation: Takasaki Radiat. Chem. Res. Establ. JAERI, Gunma, Japan, "Radiation Resistance of Polymer Composites at 77 K, Effects of Reinforcing Fabric Type, Specimen Thickness, Radiation Type and Irradiation Atmosphere," *Cryogenics*, Vol. **31**, No. **1**, Jan. 1991, pp. 7–15.

17. S. Egusa, "Irradiation Effects on/and Degradation of Mechanisms of the Mechanical Properties of Polymer Matrix Composition at Low Temperatures," *Advances in Cryogenic Engineering*, R. P. Reed and F. Fickett, eds. (Plenum Press, NY, Vol. **36**, 1990).

18. J. Bell, A. Michaels, A. Hoffman, and A. Mason, Chemical Engineering Dept., Massachusetts Institute of Technology, "Transient Acceleration of Creep Rates of Polymers During High Intensity Irradiation," Irradiation of Polymers; A Symposium, Norbert Platzer, Chairman; *Advances in Chemistry Series 66*, (American Chemical Society, Washington, D.C., 1967), pp. 79–112.

19. M. Van de Voorde, "Low Temperature Irradiation Effects on Materials and Components for Superconducting Magnets for High Energy Applications," CERN 77–03, (Feb. 1977), p. 69.

20. F. Hanisch (Kabelmetall, Hannover), P. Maier (Siemens, Karlsruhe), S. Okada (JAERI, Takasaki), H. Schonbacher (CERN); Corporate Source: (CERN), "Effects of Radiation Types and Dose Rates on Selected Cable Insulating Materials," CERN-TS-RP-191, *Radiation Physics and Chemistry*, Vol. **30**, No. **1**, March 1987, pp. 1–9.

21. G. Liptak, R. Schuler, P. Maier, H. Schonbacher, B. Haberthur, H. Muller, W. Zeir (CERN), "Radiation Tests on Selected Electrical Insulating Materials for High Power and High Voltage Applications," (CERN, Geneva, Switzerland, CERN-85-02, March 1985), p. 58.

22. T. Nishiura, S. Nishijima, K. Katagiri, T. Okada, J. Yasuda*, and T. Hirokawa*; Authors Affiliation: ISIR Osaka University, Osaka 567, Japan, and *Shikishima Canvas Co. Ltd., Ohmihachiman, Shiga 523, Japan, "Radiation Damage of Composite Materials – Creep and Swelling," *Advances in Cryogenic Engineering (Materials)*, Vol. **36**, 1990, edited by R. P. Reed and F.R. Fickett, (Plenum Press, NY), pp. 885–891.

23. R. M. AU Kurland, J. F. Thomasson, and W. C. Beggs; "Radiation Testing of Composite Materials *In Situ* Versus *Ex Situ* Effects. (Final Report)," N82-11116/2: NASA-CR-3475; REPT-351710-60288-UT-01, Nov. 1981, p. 109.

24. K. Gillen and R. Clough, Corporate Source: Sandia National Labs., Albuquerque, NM (USA), "Predicting Aging Results for Cable Materials in Nuclear Power Plants," Sandia Report, SAND90-2009, UC-523, US Government Printing Office, Nov. 1990, p. 57.

25. N. Munshi, Composite Technology Development, Inc., Boulder, Colorado, "A Radiation-Resistant Epoxy Resin System for Toroidal Field and Other Superconducting Coil Fabrication," Cryogenic Engineering Conference/International Cryogenic Material Conference, (June 1991).

26. S. Egusa, M. A. Kirk, R. C. Bircher, and M. Hagiwara; Corporate Source: Argonne National Laboratory, Div. Mat. Sci. and Technol, Argonne, IL, 60439, "Annealing Effects on Mechanical Properties of Organic Composite Materials Irradiated with Gamma Rays," *Journal of Nuclear Materials*, Vol. **127**, No. **2–3**, 1985, pp. 146–52.

27. I. S. Baishev, A. I. Drozhdin, and N. V. Mokhov, (Superconducting Super Collider Laboratory, Dallas, Texas, and Institute for High Energy Physics, Protvino, U.S.S.R), "Beam Loss and Radiation Effects in the SSC Lattice Elements," SSCL-306 (November 1990) p. 67.

28. C. Lewis Sneed and John Morena, "Radiation Testing of Superconducting Corrector-Magnet Organic Polymeric Materials," Brookhaven National Laboratory, Interim Progress Report, ATD/SSC-92-2 (December 1992).

29. "Standard Practices for Exposure of Polymeric Materials to Ionizing Radiation;" ASTM, E 1027 (1984).

30. W. L. McLaughlin, A. Miller, F. Abdelrahim, and T. Preisingeer; "Plastic Film Materials for Dosimetry of Very Large Absorbed Doses," *Radiation Physics and Chemistry* Part C, Vol. **25**, No. **4–6**, 1985, pp. 729–48.

31. W. L. McLaughlin, (National Institute of Standards and Technology); "Novel Radiation Dosimetry Systems," *High Dose Dosimetry for Radiation Processing*. Proceedings of an International Symposium, November 5–9, 1990, Vienna (Austria), (International Atomic Energy Agency, 1991, pp. 3–27, Vienna, Austria).

32. W. L. McLaughlin, (National Institute of Standards and Technology); Ba Weizhen (Academia Sinica, Xinjian (China), Xinjian Institute of Physics); H. M. Khan (Peshawar University, Peshawar (Pakistan), National Centre of Excellence in Physical Chemistry); M. Al Sheikhly, W. J. Chappas (Maryland University, College Park, MD (USA), Lab. for Radiation and Polymer Science);"Temperature Dependence of Radio Chromatic Film Dosimeters," *High Dose Dosimetry for Radiation Processing*. Proceedings of an International Symposium, November 5–9, 1990, Vienna (Austria), (International Atomic Energy Agency, 1991, pp. 305–316, Vienna, Austria).

33. V. Ritz, U.S. Naval Research Laboratory, Washington, D.C.,"F-Center Production Efficiencies at Liquid-Helium Temperature," *Physics Review (U.S)*, Vol. **130**, No. **5A**, March 1964, pp. 1452–70.

34. P. Pringsheim and P. H. Yuster, "Absorption Bands and Luminescence of LiF Irradiated at Low Temperatures," *Physical Review (U.S.)*, Vol. **78**, May 1950, p. 293.

35. W. J. Vaughan and L. O. Miller, Naval Radiological Defense Laboratory, San Francisco, "Dosimetry Using Optical Density Changes in LiF," *Health Physics,* Vol. **18**, May 1970, pp. 578–579.

36. W. L. McLaughlin, A. C. Lucas, B. M. Kapsar, and A. Miller; "Electron and Gamma-Ray Dosimetry Using Radiation Induced Color Centers in LiF," *Radiation Physics and Chemistry,* Vol. **14**, No. **3–6**, 1979, pp. 467–80.

37. M. Oberhofer (Commission of the European Communities, Ispra (Italy). Joint Research Centre [Italy], "High Level Proton Dosimetry with Thermoluminescent Materials," *Atomkernenergie*, Vol. **31**, (1978), pp. 209–216.

38. W. L. McLaughlin, A. Miller, S. C. Ellis, A. C. Lucas, and B. M. Kapsar; "Radiation Induced Color Centers in LiF for Dosimetry at High Absorbed Dose Rates," *Nuclear Instruments and Methods*, Vol. **175**, No. **1**, Sept. 1980, pp. 17–18.

39. "Standard Practices for Dealing with Outlying Observations;" ASTM, E 178 (1980).

APPENDIX A
CALCULATIONS

Superconducting Super Collider Laboratory
2550 Beckleymeade Avenue, Suite 110
Dallas, TX 75237-3946

Magnet Systems Division

MEMORANDUM

To:	**Amanda Spindel, Jon Zbasnik**	
From:	**Charles Corbett** CC	**ME04**
Date:	**3-11-92**	**92 6420 R M**
Subject:	**Documentation of G10 Pool Boiling Heat Transfer Results**	
CC:	**Don Franks, Dave Martin**	

---

1. The purpose of this memo is to document the results of the analytical heat transfer results of a 1/8"x1/8"x2.5" specimen of G10 material receiving heat energy by radiation and transfering the heat to a 1atm bath of either Helium or Nitrogen. Engineering correlations were used to calculate the temperature difference between the specimen surface and the bath temperature in either the nucleate or film boiling regimes. The maximum specimen temperature was calculated by imposing the surface temperature established from the boiling correlations (as a function of energy deposited in the block) to a 64 thermal node model of the G10 block. The assumption was made that the energy is deposited uniformly throughout the block. The steady state heat transfer was calculated using the thermal conductivity of Table 1.

2. The Kutateladze correlation was used for film boiling and the Breen and Westwater Correlation was used for film boiling. Zuber's correlations were used to predict the critical heat flux to shift from nucleate to film boiling and to predict the minimum film boiling (to return to nucleate boiling from film boiling). The effect of surface orientation was determined by work by Lyon. The above correlations and experimental results are documented in References 1 and 2. Properties used in the analysis are shown in Table 2.

3. The boiling curves for the G10 specimen in Helium is shown in Figure 1 and for Nitrogen is shown in Figure 2. The curves are plotted as energy input (watts) versus the temperature difference between the surface and the bath. The energy input reflects the effective area due to surface orientation as .9415 in^2 as opposed to actual surface area of 1.28 in^2. Using the results of the boiling curves and the thermal conductivity of Table 1, Figure 3 provides the predicted maximum specimen temperature as a function of the heat input. It can be seen from the results there is a significant temperature drop across the material itself. Heat transfer by radiation was considered negligible.

TABLE A-1. G10 THERMAL CONDUCTIVITY VS TEMPERATURE IN WARP DIRECTION.

Temperature	UNITS: w/cm-deg K vs. deg K k
4.0	0.00072
6.0	0.00099
8.0	0.00120
10.0	0.00136
15.0	0.00163
20.0	0.00182
30.0	0.00211
40.0	0.00236
50.0	0.00260
60.0	0.00284
70.0	0.00308
80.0	0.00331
100.0	0.00378
120.0	0.00423
140.0	0.00466
160.0	0.00507
180.0	0.00546
240.0	0.00649

TABLE A-2. CRYOGEN PROPERTIES USED IN CORRELATIONS.

Property	He, 1 ATM, 4.22 K	N_2, 1 ATM, 77.4 K
Vapor density – kg/m^3	16.84	4.610
Liquid density – kg/m^3	124.9	808.6
Vapor specific heat J/g-K	9.144	1.123
Liquid specific heat J/g-K	5.255	2.063
Vapor thermal cond W/m-K	0.009038	7.57e-03
Liquid thermal cond W/m-K	0.01866	0.1337
hfg J/g	20.72	198.9
Vapor viscosity – Pa sec	1.242e-06	5.26e-06
Liquid viscosity – Pa sec		151.6e-06
Surface Tension N/m	0.9944e-04	8.75e-03

References

1. E.G. Brentari and R.V. Smith, *Nucleate and Film Pool Boiling Design Correlations for O_2, N_2, H_2, and He.*
2. Steven Van Sciver, *Helium Cryogenics*, Plenum Press.

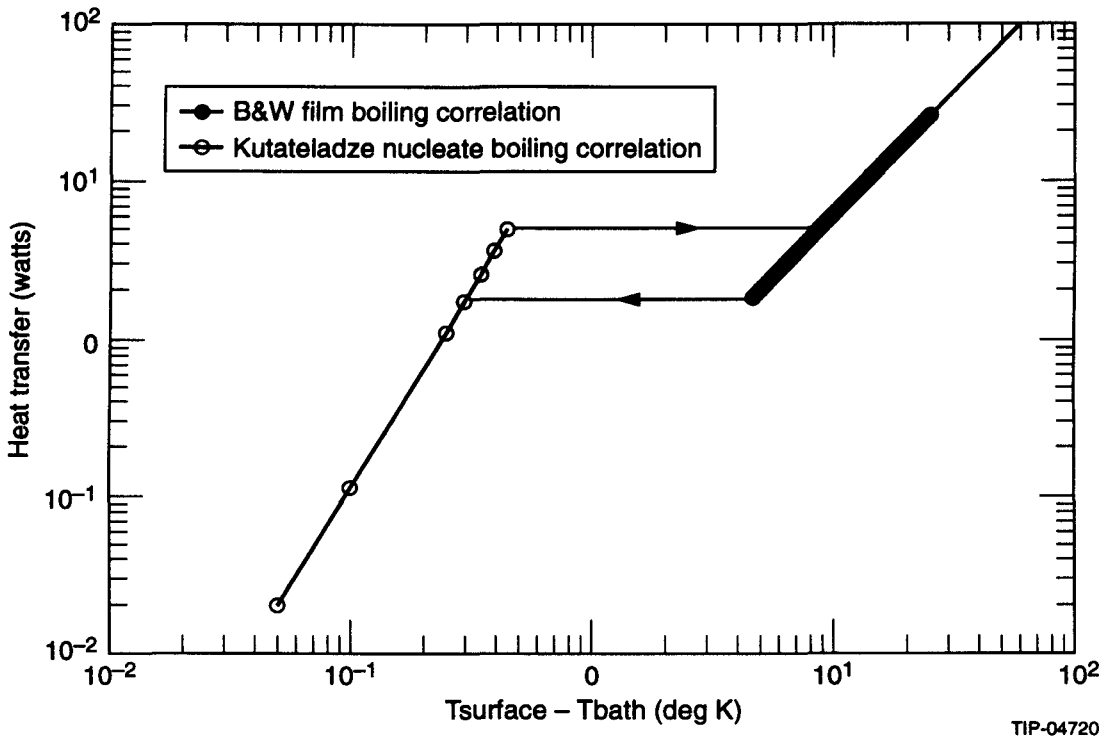

Figure A-1. Predicted Heat Transfer from a 1/8" × 1/8" × 2.5" Test Specimen in a He Bath at 1 atm and 4.222 K.

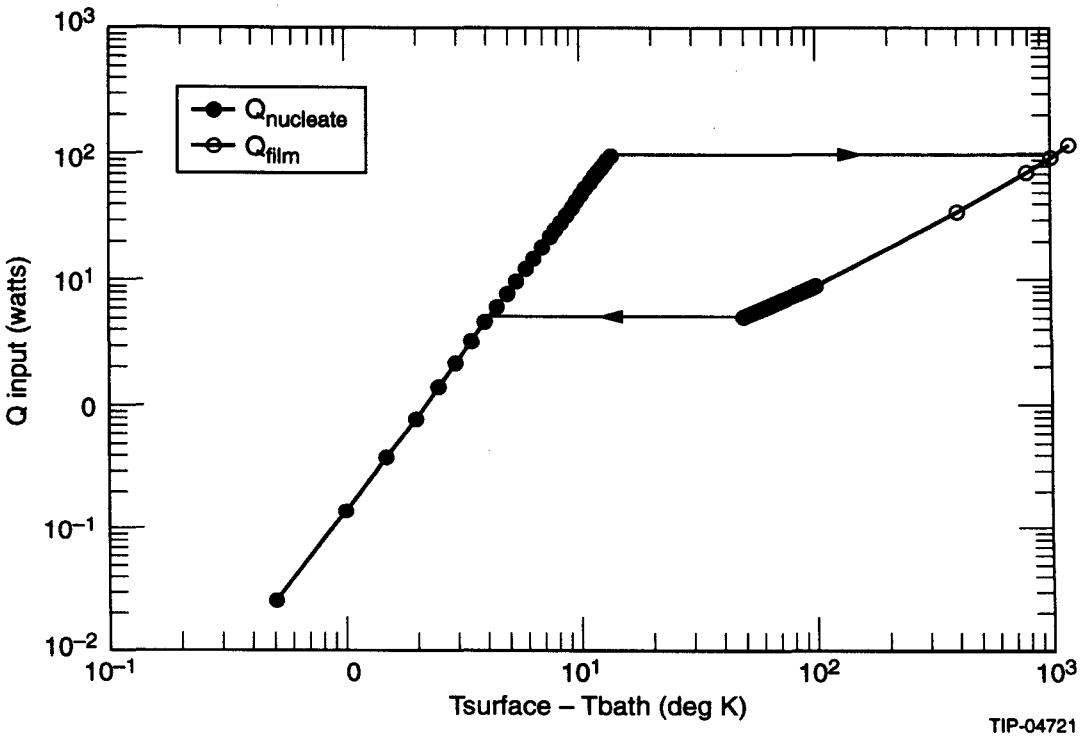

Figure A-2. Predicted N_2 Nucleate and Film Boiling for a 1/8" × 2.5" G10 Specimen in Liquid Nitrogen Bath at 1 atm and 77.4 K.

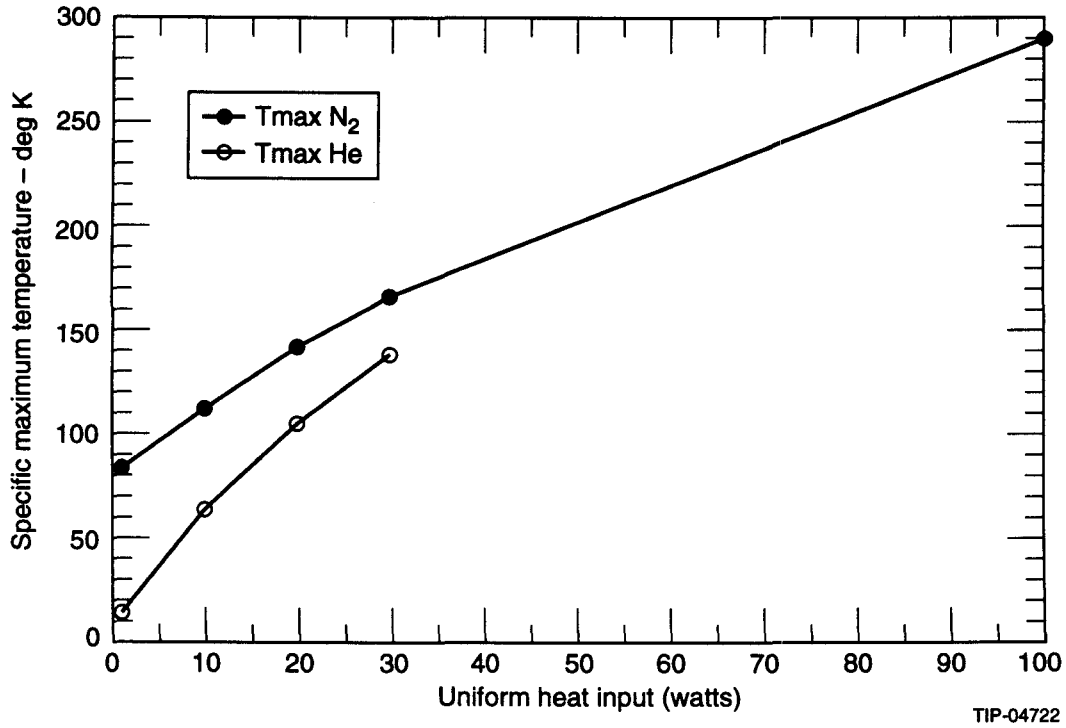

Figure A-3. Predicted Maximum G10 1/8" × 1/8" × 2.5" Specimen Temperature for Heat Transfer to a 1 atm LN_2 or Liquid He Bath under Saturated Conditions.

APPENDIX B
DATA

MATERIAL	MATL ABBR	RADS	SAMPLE #	DISPLACEMENT @ FAIL (STRAIN FOR FILMS) (IN)	STRENGTH (KSI)	MODULUS (MSI)	TYPE
ctd101g	ctd101g	0	101g_b	x	35.7	x	
		0	101g_c	0.007	35.9	1.97	
		0	101g_d	0.007	34.8	2.03	
		0	101g_e	0.006	29.8	1.94	
		10^9	36	0.005	28.3	1.94	
		10^9	37	0.001	34.1	1.79	
		10^9	38	0.005	36.1	2.34	
		10^9	39	0.001	31.4	2.16	
		10^9	40	0.006	37.4	2.17	
isryal	isryal	0	isr16	0.021	45.9	0.73	
		0	isr17	0.02	44	0.73	
		0	isr18	0.021	44.9	0.72	
		0	isr19	0.021	45.1	0.71	
		0	isr20	0.017	37.9	0.74	
		10^9	28	0.023	49.7	0.57	
		10^9	29	0.021	51.2	0.8	
		10^9	32	0.02	50.9	0.83	
		10^9	33	0.018	45.9	0.84	
		10^9	34	0.02	48.8	0.8	
		10^9	37	0.02	49.5	0.77	
		10^9	44	0.019	48	0.82	
		10^9	46	0.017	44.4	0.85	
torlon 5030	torlon	0	trin_26	0.035	59.7	1.13	
		0	trin_27	0.036	61.2	1.02	
		0	trln_28	0.036	71	1.3	
		0	trin_29	0.033	57.3	1.13	
		0	trin_30	0.036	63	1.15	
		10^9	M–1–11	0.032	60.3	1.25	
		10^9	47	0.031	57.9	1.16	
		10^9	39	0.031	62.4	1.34	
		10^9	42	0.025	47.5	1.25	
		10^9	M–7–33	0.033	61.6	1.25	
		10^9	M–6–32	0.031	64.5	1.32	
		10^9	M–0–36	0.031	59	1.25	
		10^9	M–9–35	0.032	61	1.27	
		10^9	M–3–13	0.028	54.7	1.35	
		10^9	40	0.033	57.8	1.15	
		10^9	M–4–14	0.025	52.6	1.37	
		10^9	M–5–49	0.028	53.6	1.27	
		10^9	M–8–34	0.032	60.8	1.25	
		10^9	M–2–12	0.032	59.6	1.21	
		10^9	38	x	62.4	x	
ultem 6200	ultem62	0	6200_11	0.012	29	0.81	
		0	6200_12	0.013	34.2	0.82	
		0	6200_13	0.013	33.2	0.84	
		0	6200_14	0.013	30.1	0.72	
		0	6200_15	0.015	37	0.79	
		10^9	p1	0.017	52.9	1.03	

MATERIAL	MATL ABBR	RADS	SAMPLE #	DISPLACEMENT @ FAIL (STRAIN FOR FILMS) (IN)	STRENGTH (KSI)	MODULUS (MSI)	TYPE
		10^9	p3	0.015	49.1	1.03	
		10^9	p5	0.016	48.1	0.99	
		10^8	p21	0.011	31	0.89	
		10^8	p24	0.012	33.5	0.85	
		10^9	p26	0.014	44.3	0.99	
		10^8	p45	0.012	32	0.81	
		10^8	p54	0.011	30.9	0.86	
		10^8	p57	0.013	36.4	0.87	
		10^9	p30	0.012	31.6	0.87	
		10^9	p2	0.015	50.1	1.05	
		10^8	p44	0.012	30.7	0.84	
		10^9	28	0.012	32.5	0.83	
		10^9	p4	0.016	51.2	1.01	
Envex 5630	envex	0	5630_11	0.022	31.8	0.89	
		0	5630_12	0.026	40.5	1	
		0	5630_13	0.03	54.1	1.19	
		0	5630_14	x	54.3	x	
		0	5630_15	0.021	34.7	1.1	
		10^9	b–8–23	0.034	53.9	1	
		10^9	b–0–25	0.031	46.2	0.91	
		10^9	b–6–21	0.038	70.8	1.11	
		10^8	b–32	0.032	60.2	1.15	
		10^8	b–31	0.03	53.8	1.18	
		10^9	b–7–22	0.032	60.8	1.14	
		10^8	b–33	0.034	64.1	1.13	
		10^8	b–21	0.034	51.2	0.92	
		10^8	b–3	0.032	56.4	1.07	
		10^9	b–9–24	0.028	50	1.19	
Peek	peek	0	peek16	0.016	58.2	1.13	
		0	peek17	0.017	58.9	1.03	
		0	peek18	0.017	67.3	1.19	
		0	peek19	0.018	61.1	1.01	
		0	peek20	0.015	57.6	1.19	
		10^8	42	0.016	62.9	1.31	
		10^8	43	0.015	62.1	1.29	
		10^8	44	0.014	58.6	1.33	
		10^8	45	0.015	67.1	1.46	
		10^8	e589	0.014	61.8	1.41	
		10^8	e587	0.015	60.7	1.31	
		10^8	e590	0.014	47.7	1.29	
		10^9	e7	0.017	67.8	1.24	
		10^8	e586	0.016	66	1.31	
		10^9	e2	0.013	56.3	1.32	
		10^9	e1	0.016	70.4	1.43	
		10^9	e3	0.015	64	1.36	
		10^9	e6	0.013	58.1	1.36	
		10^9	e8	0.015	66	1.42	
		10^9	e9	0.014	65.7	1.49	
		10^9	e0	0.014	64.4	1.43	

MATERIAL	MATL ABBR	RADS	SAMPLE #	DISPLACEMENT @ FAIL (STRAIN FOR FILMS) (IN)	STRENGTH (KSI)	MODULUS (MSI)	TYPE
spaulrad	spaulrad	0	spl_4a	0.045	9.9	3.14	OK
		0	spl_4b	0.038	8.9	3.47	OK
		0	spl_4c	0.045	10.2	3.51	OK
		0	spl_4d	0.041	9.5	3.54	OK
		10^9	g–8–30	0.047	10.9	3.44	OK
		10^9	g–6–29	0.043	10.32	3.63	OK
		10^9	g–7–28	0.043	10.1	3.48	OK
		10^9	g–9–23	0.045	10.21	3.66	OK
		10^9	g–0–22	0.042	9.76	3.46	OK
cryorad–p	cryoradp	0	cyp_4a	0.032	4	2.3	OK
		0	cyp_4b	0.056	4.3	2.3	OK
		0	cyp_4c	0.049	4	2.38	OK
		0	cyp_4d	0.049	4	2.39	OK
		0	cyp_4e	0.047	4.1	2.57	OK
		10^8	f26	0.051	4.5	2.57	OK
		10^8	f31	0.051	4.79	2.78	OK
		10^9	f–0–32	0.047	4.22	2.62	OK
		10^9	f–9–33	0.049	4.2	2.57	OK
		10^9	f–8–34	0.051	4.51	2.6	OK
		10^9	f–7–35	0.053	4.77	2.68	OK
		10^8	f–4–36	0.05	4.5	2.62	OK
		10^9	f–6–37	0.05	4.32	2.38	OK
		10^8	f–5–38	0.058	4.91	2.54	OK
		10^8	f–3–39	0.052	4.63	2.65	OK
me730	me730	0	me730_16	0.033	11	1.88	OK
		0	me730_17	0.036	12.2	1.95	OK
		0	me730_18	0.033	12	2.25	OK
		0	me730_19	0.032	12	2.17	BAD
		0	me730_20	0.034	12.7	2.08	OK
		10^9	c6	0.033	12.22	2.41	OK
		10^9	c7	0.032	12.42	2.42	OK
		10^9	c8	0.03	12.13	2.25	OK
		10^9	c9	0.032	11.72	2.1	OK
		10^9	c0	0.028	11.76	2.54	OK
cp1525	cp1525	0	1525_4a	x	4.6	x	OK
		0	1525_4b	x	4.4	x	OK
		0	1525_4c	x	4.5	x	OK
		0	1525_4d	x	3.9	x	OK
		0	1525_4e	x	4.3	x	OK
		10^8	18	0.029	5.24	1.91	OK
		10^8	27	0.073	4.16	1.99	OK
		10^8	k–5–16	0.025	4.87	2.14	OK
		10^8	k–1–7	0.047	5.08	1.76	BAD
		10^8	k–2–11	0.033	4.58	1.5	OK
		10^8	k–3–13	0.024	4.5	2.08	OK
		10^8	k–4–14	0.022	4.15	2.1	OK
cp1625	cp1625	0	1625_4a	x	3.8	x	OK
		0	1625_4b	x	6.5	x	OK
		0	1625_4c	x	4.8	x	OK

MATERIAL	MATL ABBR	RADS	SAMPLE #	DISPLACEMENT @ FAIL (STRAIN FOR FILMS) (IN)	STRENGTH (KSI)	MODULUS (MSI)	TYPE
		0	1625_4d	x	7.6	x	OK
		0	1625_4e	x	4.9	x	OK
		10^8	h–3–15	0.037	6.1	1.89	OK
		10^8	8	0.027	6.39	2.62	OK
		10^8	24	0.026	5.96	2.47	OK
		10^8	h–4–18	0.027	6.41	2.59	OK
		10^8	h–1–9	0.029	5.15	1.97	OK
		10^8	h–0–12	0.029	6.39	2.73	OK
		10^8	13	0.028	6.59	2.56	OK
		10^8	h–5–20	0.038	4.87	1.52	OK
Ultem 2300	ultem23	0	6	0.019	73.2	1.22	
		0	7	0.017	63	1.12	
		0	8	0.015	58.7	1.22	
		0	9	0.015	56.6	1.22	
		0	0	0.015	59.1	1.2	
		10^8	3	0.016	62.3	1.29	
		10^8	5	0.016	62.5	1.32	
		10^8	27	0.015	60.9	1.31	
		10^8	30	0.016	60.4	1.26	
		10^8	1	0.016	61.7	1.26	
		10^8	2	0.016	63	1.24	
		10^8	4	0.015	59.8	1.26	
TE630	te630	0	6	0.032	15.18	2.57	BAD
		0	7	0.047	13.59	3.69	OK
		0	8	0.048	13.87	3.8	OK
		0	9	0.051	13.65	3.68	OK
		0	0	0.046	13.17	3.78	OK
		10^9	d1	0.051	15.62	3.79	OK
		10^9	d2	0.049	13.23	3.64	OK
		10^9	d3	0.048	13.24	3.71	OK
		10^9	d4	0.047	13.28	3.73	OK
		10^9	d5	0.047	13.27	3.42	OK
Aryldite	aryldite	0	6	0.006	24.5	2.66	
		0	7	0.005	20.7	2.48	
		0	8	0.006	22.1	2.29	
		0	9	0.006	21.3	2.28	
		0	0	0.005	19.4	2.28	
		10^9	r1	x	x	x	
		10^9	r2	0.006	20.9	2.16	
		10^9	r3	0.005	10.4	2.09	
		10^9	r4	0.006	20	2.11	
		10^9	r5	0.006	18	1.94	
Vespel SP1	vespel	0	6	0.03	30.6	0.65	
		0	7	0.023	23	0.63	
		0	8	0.027	27.5	0.66	
		0	9	0.025	25.8	0.64	
		0	0	0.027	26.4	0.62	
		10^9	t1	0.019	21	0.75	
		10^9	t2	0.021	19.8	0.62	

MATERIAL	MATL ABBR	RADS	SAMPLE #	DISPLACEMENT @ FAIL (STRAIN FOR FILMS) (IN)	STRENGTH (KSI)	MODULUS (MSI)	TYPE
		10^9	t3	0.029	31.4	0.66	
		10^9	t4	0.021	21.5	0.64	
		10^9	t5	0.023	24.9	0.71	
V–388D/120 Glass (F–S)	V388/d	0	1		2.39		ADHESIVE
		0	2		2.4		
		0	3		2.26		
		0	4		2.42		
		0	5		2.76		
		10^9	1		1.34		
		10^9	2		3.08		
		10^9	3		1.73		
		10^9	4		2.51		
		10^9	5		1.52		
CTD–105(F–A)	CTD105	0	1		1.58		ADHESIVE
		0	2		1.75		
		0	3		1.35		
		0	4		2.37		
		0	5		2.34		
		10^9	1		2.05		
		10^9	2		1.8		
		10^9	3		2.17		
		10^9	4		2.09		
		10^9	5		1.88		
120C/135RCI (F–B)	ci/rci	0	1		2.31		ADHESIVE
		0	2		1.76		
		0	3		1.57		
		0	4		1.66		
		0	5		0.9		
		10^9	1		1.33		
		10^9	2		1.18		
		10^9	3		1.91		
		10^9	4		3.22		
		10^9	5		2.59		
3PM(F–D)	3pm	0	1		2.57		ADHESIVE
		0	2		1.97		
		0	3		1.7		
		0	4		2		
		0	5		2.58		
		10^9	1		2.64		
		10^9	2		1.62		
		10^9	3		2.32		
		10^9	4		1.89		
		10^9	5		2.13		
Apical NP/3P (F–J)	np/3p	0	1		2.63		ADHESIVE
		0	2		2.52		
		0	3		2.68		
		0	4		2.81		
		0	5		2.61		
		10^9	1		2.73		

MATERIAL	MATL ABBR	RADS	SAMPLE #	DISPLACEMENT @ FAIL (STRAIN FOR FILMS) (IN)	STRENGTH (KSI)	MODULUS (MSI)	TYPE
		10^9	2		1.97		
		10^9	3		2.12		
		10^9	4		1.49		
		10^9	5		1.96		
Kapton LT/3P (F–K)	lt/3p	0	1		1.15		ADHESIVE
		0	2		2.13		
		0	3		1.31		
		0	4		1.49		
		0	5		1.38		
		10^9	1		1.35		
		10^9	2		1.16		
		10^9	3		1.6		
		10^9	4		1.47		
		10^9	5		1.29		
284–46–2 Panel 1(F–N)	284462/1	0	1		1.13		ADHESIVE
		0	2		1.2		
		0	3		1.12		
		0	4		2.31		
		0	5		2.13		
		10^9	1		1.66		
		10^9	2		1.72		
		10^9	3		1.71		
		10^9	4		1.9		
		10^9	5		2.16		
284–46–2 Panel 2(F–0)	284462/2	0	1		2.02		ADHESIVE
		0	2		1.75		
		0	3		2.09		
		0	4		2		
		0	5		2.03		
		10^9	1		1.34		
		10^9	2		1.86		
		10^9	3		1.75		
		10^9	4		1.6		
		10^9	5		1.92		
135RCI/135 RCI(F–P)	rci/rci	0	1		1.05		ADHESIVE
		0	2		1.4		
		0	3		1.87		
		0	4		1.35		
		0	5		1.52		
		10^9	1		1.89		
		10^9	2		1.45		
		10^9	3		1.14		
		10^9	4		1.17		
		10^9	5		1.52		
EPVP 1037/1 (F–R)	epvp107	0	1		2.22		ADHESIVE
		0	2		1.8		
		0	3		2.19		
		0	4		2.32		
		0	5		1.81		

MATERIAL	MATL ABBR	RADS	SAMPLE #	DISPLACEMENT @ FAIL (STRAIN FOR FILMS) (IN)	STRENGTH (KSI)	MODULUS (MSI)	TYPE
		10^9	1		2.44		
		10^9	2		2.21		
		10^9	3		2.18		
		10^9	4		2.41		
		10^9	5		2.18		
EP0316(F–T)	ep0316	0	1		1.1		ADHESIVE
		0	2		1.17		
		0	3		1.08		
		0	4		0.96		
		0	5		0.82		
		10^9	1		1.08		
		10^9	2		1.25		
		10^9	3		0.87		
		10^9	4		0.91		
		10^9	5		0.85		
120xCIx140x RCI(F–V)	xci/xrci	0	1		1.66		ADHESIVE
		0	2		1.65		
		0	3		2.05		
		0	4		1.48		
		0	5		1.56		
		10^9	1		1.39		
		10^9	2		1.68		
		10^9	3		1.66		
		10^9	4		1.51		
		10^9	5		1.77		
EX1508(F–X)	ex1508	0	1		1.64		ADHESIVE
		0	2		1.65		
		0	3		1.73		
		0	4		1.61		
		0	5		1.51		
		10^9	1		1.62		
		10^9	2		1.95		
		10^9	3		1.91		
		10^9	4		1.93		
		10^9	5		1.67		
Cryorad Aprical(F–Y)	cryorad	0	1		x		ADHESIVE
		0	2		0.71		
		0	3		1.37		
		0	4		1.13		
		0	5		1.38		
		10^9	1		1.35		
		10^9	2		1.18		
		10^9	3		1.45		
		10^9	4		1.63		
		10^9	5		1.18		
Kapton LT (FC)	lt	0	2	0.049	35.78	1.01	FILM
		0	3	0.06	33.33	1.09	
		0	4	0.05	35.32	1	
		0	5	0.06	34.26	1.01	

MATERIAL	MATL ABBR	RADS	SAMPLE #	DISPLACEMENT @ FAIL (STRAIN FOR FILMS) (IN)	STRENGTH (KSI)	MODULUS (MSI)	TYPE
		0	6	x	36.64	x	
		10^9	1	0.04	32.07	1.08	
		10^9	2	0.047	33.77	1.03	
		10^9	3	0.056	35.58	1.03	
		10^9	4	0.044	32.05	1.04	
		10^9	5	0.053	36.11	1.04	
Kapton HN(FN)	hn	0	1	0.05	74.51	1.6	FILM
		0	2	0.063	68.75	1.97	
		0	3	0.082	82.06	1.55	
		0	4	0.037	66.05	1.9	
		0	5	0.054	79.19	1.72	
		10^9	1	0.049	41.12	1.01	
		10^9	2	0.047	41.52	1.02	
		10^9	3	0.055	45.84	0.99	
		10^9	4	0.047	40.05	0.98	
		10^9	5	0.071	51.29	1	
Kapton HA(FE)	ha	0	1	0.066	51.93	1.38	FILM
		0	2	0.071	48.77	1.16	
		0	3	0.06	49.57	1.22	
		0	4	0.067	51.28	1.3	
		0	5	0.067	49.29	1.44	
		10^9	1	0.074	45.42	0.85	
		10^9	2	0.067	44.52	0.89	
		10^9	3	0.075	45.13	0.82	
		10^9	4	0.074	43.79	0.84	
		10^9	5	0.07	42.03	0.8	
Kapton H(FI)	kh	0	1	0.068	61.17	1.51	FILM
		0	2	0.067	57.35	1.6	
		0	3	0.055	59.76	1.73	
		0	4	0.067	62.14	1.81	
		0	5	0.073	71.82	1.68	
		10^9	1	0.069	50.43	0.98	
		10^9	2	0.067	53.83	1.06	
		10^9	3	0.068	53.42	1.04	
		10^9	4	0.065	52.23	1.04	
		10^9	5	0.014	13.09	0.98	
Apical NP(FL)	np	0	1	0.083	74.13	xx	FILM
		0	2	0.065	61.98	1.69	
		0	3	0.071	68.54	1.82	
		0	4	0.095	68.14	1.71	
		0	5	0.072	65.33	2.09	
		10^9	1	0.063	62	1.37	
		10^9	2	0.056	58.06	1.38	
		10^9	3	0.06	62.44	1.42	
		10^9	4	0.062	60.6	1.36	
		10^9	5	0.051	55.79	1.3	
Apical AV(FM)	av	0	1	0.084	61.86	1.81	FILM
		0	2	0.1	75.57	1.71	
		0	3	0.105	63.77	2.05	

MATERIAL	MATL ABBR	RADS	SAMPLE #	DISPLACEMENT @ FAIL (STRAIN FOR FILMS) (IN)	STRENGTH (KSI)	MODULUS (MSI)	TYPE
		0	4	0.093	89.69	1.62	
		0	5	0.107	77.9	1.91	
		10^9	1	0.084	47.13	0.92	
		10^9	2	0.127	47.94	0.94	
		10^9	3	0.079	51.88	1.02	
		10^9	4	0.128	51.6	0.98	
		10^9	5	0.094	56.22	0.98	
VTEM1	vtem1	0	6	0.031	11.81	2.34	OK
		0	7	0.05	9.89	2.25	OK
		0	8	0.062	8.51	2.66	OK
		0	9	0.062	8.35	2.74	OK
		0	0	0.067	8.88	2.76	OK
		10^9	a1	0.065	8.72	2.87	OK
		10^9	a2	0.065	8.88	3.31	OK
		10^9	a3	0.063	8.63	3.33	OK
		10^9	a4	0.061	8.23	3.15	OK
		10^9	a5	0.063	8.38	2.93	OK
		10^8	a94	0.065	8.98	3.4	OK
		10^8	a95	0.064	8.48	3.14	OK
		10^8	a97	0.061	8.33	3.18	OK